Fall 12-11-2017

The Impact of Reduced Arctic Sea Ice Extent on Cryospheric Snowfall

Alexander Carne
University of Nebraska-Lincoln, alexander.carne@huskers.unl.edu

THE IMPACT OF REDUCED ARCTIC SEA ICE EXTENT ON CRYOSPHERIC SNOWFALL

by

Alexander R. Carne

A THESIS

Presented to the Faculty of
The Graduate College at the University of Nebraska
In Partial Fulfillment of Requirements
For the Degree of Master of Science

Major: Earth and Atmospheric Sciences

Under the Supervision of Professor Mark Anderson

Lincoln, Nebraska

August, 2017

THE IMPACT OF REDUCED ARCTIC SEA ICE EXTENT ON CRYOSPHERIC SNOWFALL

Alexander Richard Carne, M.S.
University of Nebraska, 2017
Advisor: Mark R. Anderson

Satellite observations show that sea ice extent in the Arctic has been declining from 1979 through present day, reaching record minimum extents in 2007 and 2012. Reduced sea ice extent allows for greater expanses of open water to interact with the Arctic atmosphere, potentially leading to changes in the Arctic climate. The greatest declines in Arctic sea ice extent have occurred in summer and autumn. During these seasons, it is likely that the decrease in Arctic sea ice extent led to an increase in atmospheric sensible and latent heat fluxes, possibly leading to increases in Arctic temperature and moisture. Increases in atmospheric temperature and moisture would likely impact Arctic precipitation patterns, and if the temperature is cold enough, snowfall would be impacted as well. Investigations into the impact of reduced sea ice extent on Arctic snowfall has been conducted over seasonal time scales, however, a lack of attention has been given to the influence of reduced Arctic sea ice extent on snowfall within individual cyclones. This study examines the impact of reduced Arctic sea ice extent on snowfall produced within individual Arctic cyclones through a reanalysis study. The autumnal months of October and November are examined for the years 1982 and 1985, years that possess normal to above normal sea ice extents compared to 2007 and 2012, years that possess

below average sea ice extents. Additionally, monthly snowfall and snow depth are examined to provide a comparison of the seasonal scale snowfall patterns during October and November of the four years. Data for analysis are produced by running the Weather Research and Forecasting Model (WRF) utilizing the European Center for Medium Range Weather Forecasting (ECMWF) ERA-Interim reanalysis dataset in an Arctic domain. Results indicate that locations along the Arctic coast, along with ice-covered regions near the sea ice margin, have the greatest potential for increased snowfall and snow depth from high-latitude cyclones. The results also suggest that monthly snowfall increases over the Arctic Ocean in October with reduced Arctic sea ice, leading to an increase in snow depth over existing multi-year sea ice in years with below average sea ice extents.

TABLE OF CONTENTS

ACKNOWLEDGEMENTS

I would first like to thank my thesis advisor Dr. Mark Anderson of the department of Earth and Atmospheric Sciences at the University of Nebraska-Lincoln (UNL). The door to Dr. Anderson's office was always open whenever I ran into a trouble or had a question about my research, and he was very approachable when I needed help. He guided me in the right direction when I needed aid, but also challenged me to resolve problems on my own.

I would also like to thank my committee members Dr. Clinton Rowe and Dr. Robert Oglesby of the department of Earth and Atmospheric Sciences at UNL. Their input on my research was greatly appreciated, especially with their help in setting up the WRF model. Whey worked with me to assure that my model parameters were set correctly to allow for a successful simulation of the Arctic environment. I would additionally like to extend thanks to Cindy Hays of the Department of Natural Resources at UNL, who provided technical support when I ran into trouble running WRF or NCL. She was always very quick to respond when I had an issue, and always provided a helpful answer.

I would finally like to acknowledge my family, who provided support and encouragement through the entire process. I would not have been able to do it without you, and I sincerely thank you for all that you have done.

Alexander Carne

CHAPTER 1: INTRODUCTION

Earth's climate system is experiencing dramatic changes due to anthropogenic global warming. The average global temperature has risen 0.94˚C through 2016 compared to the 20th century average, with much of the warming occurring since 1970 (National Centers for Environmental Information 2017). This warming is leading to rising sea levels, retreating glaciers, declining sea ice, and greater extremes in temperature and precipitation (National Snow and Ice Data Center 2017, National Centers for Environmental Information 2017). Global warming has become a widely-recognized threat to the planet, though much is still not understood about its effects. Anthropogenic global warming is primarily caused by an increase in greenhouse gas concentrations in the atmosphere. The warming caused by human activity leads to a variety of feedbacks that impact the climate. These feedbacks have attracted researchers, as they are key to understanding the future impacts of climate change.

The ice-albedo feedback makes the Earth's cryosphere particularly sensitive to the impacts of climate change (Stone et al. 2002). Arctic sea ice extent has been declining over recent decades, with a record minimum sea ice extent of 3.4×10^6 km^2 recorded in September 2012. This is only 53% of the 1979-2013 average of 6.4×10^6 km^2 (Parkinson 2014). As the extent of sea ice declines, the average surface albedo in the Arctic decreases, allowing for greater absorption of incoming shortwave radiation and further warming of the cryosphere (Deser et al. 2010). This leads to Arctic temperature

amplification, where melting glaciers and declining sea ice extent enhance the warming in the cryosphere (Simmonds and Screen 2010). Reduced sea ice extent will also increase the sensible and latent heat fluxes between the Arctic Ocean and atmosphere (Simmonds and Keay 2009). The impacts of increased atmospheric heat and moisture are not well understood, particularly the impacts on precipitation and snowfall patterns across the Arctic. Previous studies have considered the impact of declining sea ice extent on snowfall over seasonal time scales (Liston and Hiemstra 2011, Wegmann et al. 2015), though there has been a lack of discussion on impacts occurring within individual cyclones.

This study investigates the impact of reduced Arctic sea ice extent on snowfall totals within individual cyclones during the autumn season, hypothesizing that a decrease in autumnal Arctic sea ice extent will lead to an increase in snowfall production within high-latitude cyclones due to an increase in atmospheric temperature and moisture. An analysis is conducted to observe patterns of snowfall and snow depth, focusing on a study domain stretching eastward from north-central Siberia to the Yukon Territory, and northward from the Kamchatka Peninsula to near the North Pole (Figure 1.1). A case study analysis investigates snowfall patterns within three particular case studies, comparing cyclones over differing sea ice extent environments. Additionally, monthly snowfall and snow depth are analyzed. The months of October and November are chosen for study as sea ice extent has remained low after the September sea ice minimum in recent years, and snowfall becomes a regular occurrence in the Arctic as the region transitions into the cold season. The Weather Research and Forecasting Model (WRF)

(Skamarock et al. 2008) is run using the Era-Interim reanalysis dataset (Dee et al. 2011) to produce snowfall data for this analysis.

In addition to the lack of prior research, additional motivation for this study comes from the sensitivity of the Arctic system to changes in snow cover. Snow cover acts as an insulator to the surface below, increases longwave radiation emissivity, and possesses a high surface albedo (Krasting et al. 2013). These properties of snow cover all lead to a cooling of the near-surface air. Additionally, an increase in snowfall may impact the Arctic hydrologic cycle (Bengtsson et al. 2011), the ice mass balance of glaciers (Singarayer et al. 2006), the freeze-thaw cycle of lake and sea ice (Hezel et al. 2012), and large-scale teleconnection patterns (Cohen et al. 2012).

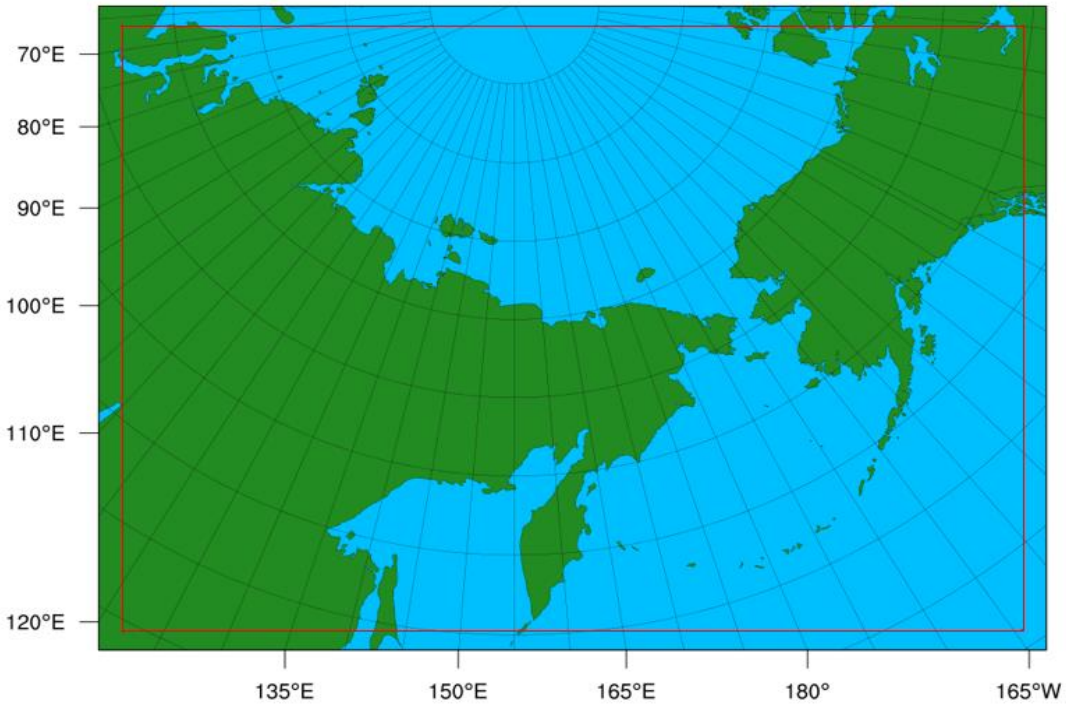

Figure 1.1.

WRF domains utilized in the study, the parent domain (Domain 1) forms the perimeter of the map while the nested domain (Domain 2) is highlighted by the red box

CHAPTER 2: BACKGROUND

It is suggested that sea ice extent decline is leading to changes in Arctic snowfall (Räisänen 2008). This apparently is because decreases in sea ice extent in the Arctic will have an impact on energy fluxes between the open ocean and atmosphere (Deser et al. 2010), which would lead to changes in temperature (Singaryer et al 2006) and moisture (Liua et al. 2012) in the Arctic. Changes in temperature and moisture could alter cloud cover (Eastman and Warren 2010) and precipitation (Räisänen 2008), along with autumnal snowfall patterns (Schweiger et al. 2008).

2.1 Arctic sea ice decline and coverage

Sea ice extent in the Arctic Ocean basin typically reaches a maximum in March and minimum in September. The average sea ice extents for March and September are approximately 15.5×10^6 km^2 and 6.4×10^6 km^2, respectively (National Snow and Ice Data Center 2017), based on observations from 1981-2010. Sea ice will be present across most of the Arctic Ocean basin in the winter months, with lower latitude portions of the Arctic Ocean becoming ice-free during the warm season. The inter-annual variability of Arctic sea ice extent is greatest near the September minimum (Simmonds and Keay 2009). This allows for a high variability in the amount of open ocean available to interact with the atmosphere above the Arctic Ocean in late summer and early autumn. Summer Arctic sea ice is sensitive to the impacts of global climate change, and the decline in warm-season Arctic sea ice extent has been shown to be the leading factor in Arctic temperature amplification (Simmonds and Screen 2010). This has allowed mean surface air temperature in the Arctic to rise at nearly double the average global rate. (Simmonds

and Screen 2010). With greater increases in temperature occurring in the Arctic, warm-season Arctic sea ice extent will continue to decline (DeRepentigny et al. 2016), potentially leading to further climate feedbacks in the Arctic.

Satellite observations show that Arctic sea ice extent is decreasing, with the greatest declines occurring in summer and autumn (National Snow and Ice Data Center 2017). The decline of minimum Arctic sea ice extent has accelerated from 7% per decade from 1979-2001 to 14% per decade by 2013 (Stroeve et al. 2014). Regions within the Arctic Ocean basin that have experienced the greatest rates of sea ice decline through the mid-2000's includes the Barents and Kara Seas (Sorteberg and Kvingedal 2006), and near the northern coasts of Alaska, Canada, and Greenland, as well as in Fram Strait (Lindsay and Zhang 2005). In addition to a downward acceleration of minimum sea ice extents, sea ice thickness and the proportion of multi-year ice have also been declining (Stroeve et al. 2014). The proportion of multi-year ice in the Arctic, which tends to be thicker than seasonal ice, has dropped from 70% to 20% of the total Arctic sea ice extent between the mid-1980s to 2012 (Stroeve et al. 2014). Sea ice volume takes longer to recover than sea ice extent (Sedláček et al. 2012), making it more difficult to replace thicker multi-year ice in a warming climate. The length of the melt season has also been increasing in the Arctic at a rate of 5 days per decade (Stroeve et al. 2014). If these trends continue, Arctic sea ice extent will continue to decline. A "business as usual" scenario of greenhouse gas increases would yield an ice-free warm-season Arctic Ocean by the year 2100 (DeRepentigny et al. 2016). If the Arctic Ocean continues to trend toward an ice-free warm season, a larger amount of open ocean will be available to interact with the atmosphere than previously. The climatic impact of these new open waters may be

substantial, especially on precipitation and snowfall over the Arctic Ocean and adjacent landmass, thus further research into the impact of Arctic sea ice decline on Arctic snowfall is needed.

2.2 Arctic Temperature and Radiative Fluxes

The decline in Arctic sea ice extent is leading to dramatic changes in both the regional and global climate. The 2007 sea ice minimum left the Arctic Ocean with 3×10^6 km^2 of anomalous open water. For reference, the total surface area of the Great Lakes, which has a very strong impact on the local climate, is only 2.43×10^5 km^2 in area (Strey et al. 2010). The net radiative flux across the Arctic Ocean is upward during the cold season, and downward during the warm season (Beesley 2000). Warm-season sea ice decline allows for a larger area of open water to interact with the atmosphere, allowing for an increase in sensible and latent heat fluxes across the Arctic (Deser et al. 2010). The greatest increases in turbulent energy fluxes (the sum of latent and sensible heat fluxes) from the ocean surface to the atmosphere occur in November, about a month and a half after the minimum Arctic sea ice extent (Deser et al. 2010). It also appears that the peak magnitude in latent heat flux into the atmosphere is occurring slightly earlier than the peak in sensible heating (Screen et al. 2013). Temperature and precipitation responses to sea ice decline are in temporal alignment with turbulent energy fluxes, rather than sea ice extent (Deser et al. 2010). The greatest impact of sea ice decline on the Arctic climate will therefore occur in mid to late autumn, as opposed to late summer when the minimum sea ice extent occurs. This supports the autumn time domain used here for investigating the impact of Arctic sea ice extent decline on high-latitude snowfall.

The maximum increase in surface-to-atmosphere turbulent heat flux has been over 40 Wm^{-2} compared to turbulent heat fluxes under normal sea ice conditions (Strey et al. 2010), with average increases of near 2.5 Wm^{-2} across the full Arctic Ocean basin (Screen et al. 2013). Surface to atmosphere turbulent energy fluxes may increase by up to 65-70 Wm^{-2} by the end of the 21st century, relative to fluxes under current average sea ice conditions (Deser et al. 2010). The largest increases in latent and sensible heat fluxes are occurring in regions experiencing the greatest sea ice decline (Screen et al. 2013), with robust increases in turbulent energy fluxes occurring over a small geographic area near the sea ice margin (Alexander et al. 2004). It is therefore likely that the greatest changes in Arctic precipitation and snowfall will occur near the sea ice margin. In addition to an increase in upward turbulent energy fluxes in winter, shortwave radiation absorption is increasing during the Arctic warm season due to declining sea ice (Deser et al. 2010). The increase in energy absorbed by the Arctic Ocean during the warm season may lead to a later freeze-up of autumnal sea ice if some of the energy remains in the ocean through autumn (Francis et al. 2009).

Increasing surface-to-atmosphere sensible and latent heat fluxes allows for an increase in atmospheric temperature over the Arctic Ocean, particularly near the sea ice margin. Consistent with the maximum increase in surface-to-atmosphere turbulent energy fluxes, the maximum increase in temperature occurs in November (Deser et al. 2010). When isolating sea ice decline as a forcing, projected November temperature increases are as high as 17˚C near the late 21st century sea ice margin (Deser et al. 2010). End-of-the-century annual temperature increases are projected to be between 3˚C and 4˚C averaged across the Arctic Ocean, with much of this warming occurring during the cold season

(Singaryer et al 2006). Most of the warming from sea ice decline is projected to occur in the lower atmosphere (below 700 hPa) and remain in the local Arctic region (Singarayer et al. 2006). This may mean that changes in snowfall from sea ice decline could remain confined to the Arctic regions. The increased heat input into the lower atmosphere from sea ice decline will also influence the low-level boundary layer, by increasing the boundary layer depth (Francis et al. 2009) and decreasing the strength of the surface inversion during the cold season (Screen et al. 2013). The increase in boundary layer depth allows for low-level thermal energy to be stored in a greater mass of atmosphere, further delaying the freezing of autumnal sea ice (Francis et al. 2009).

2.3 Changes in Arctic moisture and cloud cover

The decreases in Arctic sea ice extent are also leading to changes in Arctic moisture and cloud cover patterns. Along with an increase in temperature, increasing sensible and latent heat fluxes over regions of sea ice decline are leading to an increase in atmospheric moisture over the Arctic Ocean (Liua et al. 2012). The moisture source for Arctic precipitation shifts from locally driven during the warm season, to a dependence on remote moisture transport during the cold season with the freeze-up of the Arctic Ocean (Kurita 2011). This shift will occur later if the Arctic sea ice extent takes longer to build up in autumn due to anthropogenic climate change. The amount of moisture increase that is directly due to a decrease in sea ice decline is more difficult to determine than temperature. Moisture advection from lower latitudes will impact the amount of moisture present in the Arctic. Additionally, the Clausius-Clapeyron relationship will impact moisture content in the Arctic atmosphere, increasing moisture holding capacity in the air as the temperature of the Arctic increases. The Clausius-Clapeyron relationship will, on

average, lead to a 6-7% increase in moisture capacity with every 1˚C increase in temperature due to the higher saturation vapor pressure with increasing temperature (Bengtsson et al. 2011). The increase in ocean-to-atmosphere latent heating, along with warming temperature via the Clausius-Clapeyron relationship, are the primary reasons for the observed increase in Arctic moisture (Cohen et al. 2012).

The increases in temperature and moisture from sea ice decline across the Arctic Ocean basin are having an impact on cloud cover across the region. There seems to be a lack of consensus on the impact of sea ice decline on Arctic cloud cover, particularly with the potential changes in low-level stratiform cloud cover. One hypothesis is that a decrease in autumnal Arctic sea ice will lead to a decrease in low-level stratiform clouds, while increasing mid-level clouds (Schweiger et al. 2008). This hypothesis is driven by a weakening of the boundary layer inversion in a warmer Arctic, decreasing low-level stratiform cloud coverage. It is alternatively hypothesized that decreases in Arctic sea ice will increase the coverage of low-level stratiform clouds (Eastman and Warren 2010), driven by an increase in low-level moisture over anomalously ice-free portions of the Arctic. Low-level clouds are an important feature for the Arctic climate, as they produce a strong downward radiative forcing, allowing the Arctic boundary layer to stay warmer during the cold season when clouds are present. An increase in low-level clouds could act to further delay the freeze-up of autumnal sea ice if the temperature remains elevated during the transition into the cold season. Additionally, it is hypothesized that if low-level clouds increase due to a decrease in sea ice extent, a decrease in the proportion of precipitating clouds in the Arctic may result, with this impact most prominent in autumn

(Eastman and Warren 2010). This implies that potential increases in moisture and cloud cover will not always lead to more precipitation.

2.4 Changes in Arctic general circulation, teleconnections, and storm tracks

Declining sea ice extent along with ambient climate change is leading to changes in Arctic atmospheric circulation patterns, along with consequent changes in high-latitude cyclone behavior (DeRepentigny et al. 2016, Simmonds and Keay 2009). The Arctic Oscillation (AO) is a primary mode of atmospheric variability in the Northern Hemisphere. The positive phase of the AO produces decreased sea level pressure in the Arctic and increased sea level pressure in mid-latitude regions (Holland 2003), which leads to a more zonal upper-level flow regime across the Northern Hemisphere, while the negative phase of the AO produces increased sea level pressure in the Arctic and a more amplified upper-level wave pattern. Studies on the impact of sea ice decline on the AO are conflicting. Some studies suggest that sea ice extent decline will allow for a tendency toward the positive phase of the AO (DeRepentigny et al. 2016, Yin 2005), while others find that a negative phase AO would be favored with sea ice extent decline (Liua et al. 2012). The North Atlantic Oscillation (NAO), which is partially encompassed by the AO, is another leading mode of atmospheric variability in the Northern Hemisphere (Holland 2003). A negative trend in the NAO is favored to occur with declining sea ice (Sedláček et al. 2012, Francis et al. 2009), though as was the case with the AO, a great deal of uncertainty exists with future patterns of the NAO. A higher 500 hPa wave number has been found to occur in years with lesser Arctic sea ice extent, leading to a tendency toward meridional flow and greater chances for blocking patterns to develop

(Wegmann et al. 2015). Changes in teleconnection patterns can impact cyclone behavior across the Arctic, leading to potential changes in precipitation and snowfall.

The decline of Arctic sea ice extent is also having an impact on surface cyclone activity throughout the Arctic. A reanalysis study from 1979-2008 finds that average Arctic cyclone depths and radii are increasing by 1.58 hPa per century and 0.7˚ latitude per century (Simmonds and Keay 2009). This may be due to an increasing potential for baroclinicity in an environment possessing an increasing proportion of open ocean. Future projections bring cyclone tracks poleward during the cold season, which would lead to a poleward shift in precipitation patterns (Yin 2005). An analysis of cyclone activity from 1948-2002 finds that cyclone activity has increased across the Arctic, with a greater number and strength of cyclones traveling from mid-latitudes into the Arctic (Zhang et al. 2004). This would also cause a poleward shift in Northern Hemisphere storm tracks. It is additionally suggested that the strength of the Siberian high will increase in relation to a decrease in cold-season Arctic sea ice extents, along with decreasing surface temperature near the center of the high (Wu et al. 2011). This could potentially result from a displacement of cold air from the Arctic Ocean into the Eurasian continent, with anomalously reduced sea ice extents allowing for a warmer atmosphere over the Arctic Ocean.

2.5 Changes in Arctic precipitation

Many of the changes to the Arctic system discussed so far will likely influence precipitation in the Arctic. Warmer temperature, higher moisture, and more cyclones tracking through the Arctic are all likely to lead to greater precipitation. At seasonal to annual time scales, the influence of sea ice extent decline on Arctic precipitation has

received abundant attention from researchers. Most studies have found that precipitation is increasing in the Arctic in response to climate change and sea ice decline (Deser et al. 2010, Räisänen 2008, Singarayer et al. 2006). It is projected that the entirety of the high-latitude Arctic will experience increases in precipitation through the 21st century (Räisänen 2008). Projected increases in mean daily precipitation due to sea ice decline range from 0.15 mm per day (Singarayer et al. 2006) to 0.4 mm per day (Deser et al. 2010) by the end of the 21st century, averaged over the Arctic. The greatest increases in precipitation are expected to occur near the sea ice margin (Singarayer et al. 2006), in spatial alignment with the greatest increases in sensible and latent heat fluxes. Some uncertainty exists in the magnitude and geographic distribution of the changes in precipitation, as a large regional variation in precipitation changes is noted in a study of past precipitation patterns in the Arctic (Hinzman et al. 2005).

It also appears possible that a greater turnover (an acceleration) of the hydrologic cycle will occur over the Arctic Ocean, as evaporation and precipitation are both expected to increase with declining sea ice. Changes in the ratio of evaporation to precipitation can impact freshwater deposits over both oceanic and continental regions, causing a wide range of impacts including disrupted ocean currents and an alteration of glacial ice mass balance (Singarayer et al. 2006). The consensus among studies is that precipitation is increasing in the Arctic due to sea ice decline (Deser et al. 2010, Räisänen 2008, Singarayer et al. 2006). It is less well understood how these increases in precipitation will occur within individual cyclones in the Arctic, particularly the impact on snow precipitation within high-latitude cyclones.

2.6 Changes in Arctic snowfall

Snowfall is dependent on many factors that include; snow water equivalent, atmospheric column temperature, surface temperature, vertical extent of forcing for ascent, and wind velocity. A pair of storms that produce equal amounts of liquid water equivalent have the potential to produce vastly differing snowfall totals, even if all precipitation falls as snow. It appears that the fraction of precipitation days producing snowfall in the Arctic is decreasing, most notably during the transition seasons due to a greater proportion of precipitation events producing rain (Liston and Hiemstra 2011). Precipitation is increasing in the Arctic (Deser et al. 2010), which increases Arctic snowfall when the temperature is cold enough for snow (Krasting et al. 2013). These two factors will likely determine the changes in Arctic snowfall, especially during the autumn season.

Studies find that changes in Arctic snowfall range from nearly stationary to increasing. From 1979-2009, it is found that average annual snowfall totals remain nearly unchanged in the Northern Hemisphere from 55˚ N to 90˚ N (Liston and Hiemstra 2011), but with a decline in the number of days observing snowfall. Other studies indicate an increase in snowfall occurring during the full cold season (Räisänen 2008) and during autumn (Schweiger et al. 2008). Almost the entire Northern Hemisphere experiences a decline in snowfall during the beginning and end of the snow season, with a potential increase in snowfall occurring during the core of the cold season (Krasting et al. 2013). High-latitudes have a greater chance at annual snowfall increases as the increases in snowfall due to greater cold season precipitation totals will likely be larger in magnitude than the decreases in transition-season snowfall due to warming temperatures (Räisänen 2008).

Mid-latitude regions are likely to experience a decrease in seasonal snowfall, with the -20˚C November-March average isotherm roughly dividing the regions experiencing increases from those experiencing decreases in annual snowfall.

The analysis of snow depth across the Arctic is different than the evaluation of snowfall. Snow depth is dependent on variables including the input of snowfall, and snow loss due to melting, sublimation, and compaction of existing snow cover (Kapnick and Delworth 2013). This means that changes in Arctic snowfall climatology may differ from changes in snow depth climatology. It is forecast that snow depth will increase across high-latitude continental regions through the end of the 21st century, with average snow depth increases of 1.5-3 cm liquid equivalent occurring by the start of the spring melt season in Siberia, and increases of 1-1.5 cm occurring in northern Alaska and northern Canada by the start of the melt season (Deser et al. 2010). Additionally, observations from 1988-2012 show that October snow depth across the Eurasian continent has increased (Cohen et al. 2012).

The decrease in snowfall at the start of the snow season (September) does not look to be causing a decrease in snow depth, as snow depth is increasing in many regions, likely due to an increase in mid to late autumn snowfall. The impacts of an increase in high-latitude snow depth are diverse, and affect both the regional and global climate. Snow is a poor conductor of heat due to a high air content within a snowpack (Warren et al. 1999). Additionally, the high albedo of snow will absorb less incoming shortwave radiation in spring. These factors allow a deeper snowpack to promote a cooling of the Arctic climate relative to the ambient warming. It has even been suggested that the increases in Siberian snow depth have canceled out the otherwise background warming in

winter, leading to a near zero change in cold-season temperatures over the period from 1988-2010 (Cohen et al. 2012). Autumnal snowfall variability also has the potential to force the wintertime phase of the AO, creating impacts to climate at a global scale (Cohen et al. 2012). In addition to influencing temperature, changes in high-latitude continental snow depth have the potential to alter the hydrologic cycle by increasing the turnover of the water cycle, leading to the aforementioned impacts on Arctic freshwater distribution and glacial ice mass balance (Singarayer et al. 2006). An increase in snow depth on Arctic sea ice can lead to impacts on the thickness and distribution of sea ice. The insulating properties of snow cover can slow both the growth of Arctic sea ice thickness in autumn and the melting of sea ice in spring (Warren et al. 1999).

Prior studies have not focused on the relationship between Arctic sea ice extent and snowfall at smaller time scales, within individual cyclones, necessitating investigation into this topic. It is evident that temperature and moisture are increasing in the Arctic (Simmonds and Screen 2010), partially due to an increasing sensible and latent heat flux in the region (Deser et al. 2010). Additionally, it appears that cyclone tracks are shifting poleward (Yin 2005), and increasing in average strength (Simmonds and Keay 2009) in the Arctic. Finally, precipitation and snowfall are increasing during at least a portion of the cold season (Räisänen 2008), with these increases allowing for an increase in high-latitude continental snow cover (Cohen et al. 2012). This background evidence leads to the hypothesis for this study: a decrease in autumnal Arctic sea ice extent will lead to increasing snowfall within high-latitude cyclones.

CHAPTER 3: METHODOLOGY

3.1 Experiential procedure

Using the WRF, a case study analysis is conducted to observe the impacts of reduced Arctic sea ice extent on snowfall totals produced from high-latitude cyclones in autumn. Each case will consist of two cyclones, one from a year with a below average sea ice extent, and one from a year with greater sea ice extent relative to the first cyclone. Cyclones selected for analysis will have tracks that either overlap or come close to overlapping. In addition to the case studies, monthly total snowfall and snow depth are analyzed to provide a comparison of the seasonal scale snowfall patterns during October and November of the studied years. The goal is to isolate sea ice extent as the dominant forcing for changes in snowfall, where sea ice extent is defined as the region inside the 15% sea ice extent isopleth. The data used for the study are taken from October and November of the years 1982, 1985, 2007, and 2012.

The year 1982 has an above average autumnal sea ice extent in the Arctic, relative to the 1981-2010 average, while 1985 has a near average autumnal sea ice extent (National Snow and Ice Data Center 2017) (Figure 3.1). In both years, most of the Russian and Alaskan coastlines are ice-covered by the end of October, though differences are found in the Kara Sea, where only 1982 experiences sea ice coverage in late October. Both years provide cyclone examples in an environment where ample ice coverage exists along the Asian and Alaskan coasts. The years 1982 and 1985 will act as the “normal” sea ice extent years in this study and will be represented by “N” during the case study analysis. Below average autumnal sea ice extents occur in 2007 and 2012 relative to the 1980-2010

average, and these years hold the records for the lowest and second lowest, respectively, minimum sea ice extents on record since 1979 (National Snow and Ice Data Center). A large region of anomalous open water is found off the Arctic coastline of North America in late October 2012, while the Chukchi Sea is anomalously devoid of sea ice near the end of October 2007. This allows for more interaction between the unfrozen ocean and atmosphere above. The years 2007 and 2012 will act as the "reduced" sea ice extent years and will be represented by "R" in the case study analysis.

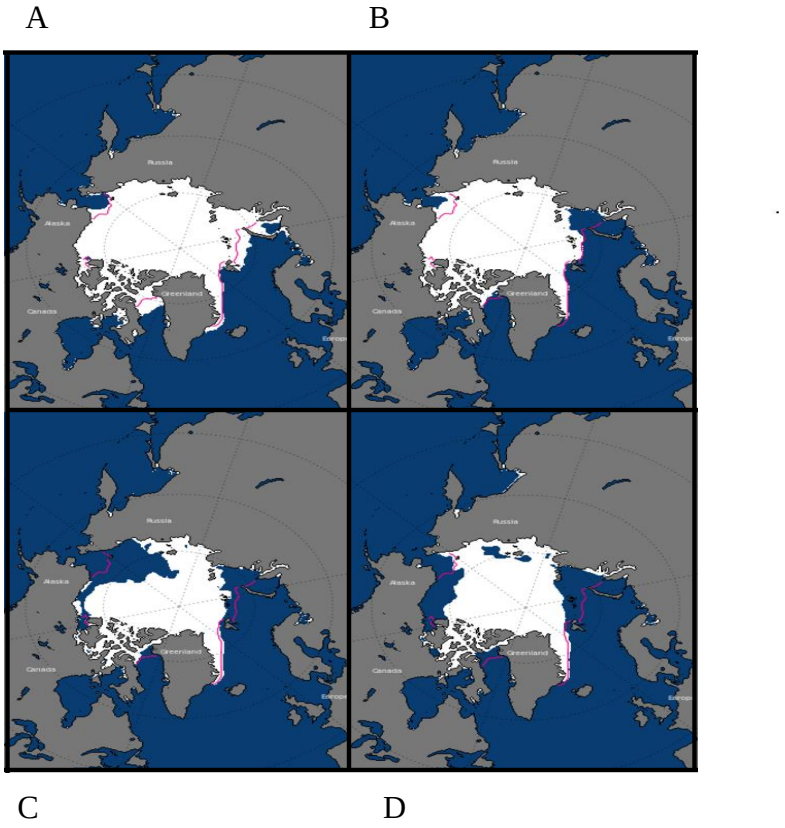

Figure 3.1.

Sea ice coverage and extent (white area) and 1981-2010 median ice edge (pink contour) for 00 UTC 30 October for the years; (A) 1982, (B) 1985, (C) 2007, and (D) 2012 (National Snow and Ice Data Center 2017).

3.2 WRF Model setup and run

The WRF version 3.7.1 (Skamarock et al. 2008) is run to simulate the Arctic atmospheric conditions and snowfall amounts since observations in these regions are not adequate for the level of detail required for this analysis. The WRF version 3.7.1 possesses a series of updates that make the model appropriate for research within a polar domain. A fractional sea ice feature was added in WRF version 3.1 onward to allow sea ice concentration to vary, and the Noah land surface model has been updated to allow for improved energy transfer between ice-covered surfaces and the Arctic atmosphere. Sea ice albedo is set to 0.65, with sea ice thickness at 3 m where sea ice is present.

WRF is run utilizing the ERA-Interim reanalysis dataset for large scale forcing (Dee et al. 2011). The ERA-Interim reanalysis dataset is derived from the European Center for Medium-Range Weather Forecasts (ECMWF) model. ERA-Interim data extend from 1979 through 2016, and are updated frequently to bring data up to near-present date, providing gridded data available for WRF input on a 6-hourly basis. The ERA-Interim reanalysis dataset is chosen for this study as data exist for the high Arctic domain utilized in this study, and provide adequate temporal resolution for case study analysis. The sea ice and sea surface temperature data are derived from the ERA-Interim reanalysis dataset and come from different sources, including the NCEP 2-DVar analysis in 1982 and 1985, the daily operational NCEP sea ice concentration product in 2007, and the operational sea surface temperature and sea ice analysis (OSTIA) in 2012 (Dee et al. 2011, Fiorino 2004).

The WRF model simulations consist of a 12×12 km domain nested within a 36×36 km domain on a polar projection. The model is run over a 5-month period, beginning at 00 UTC 1 August and ending at 00 UTC 2 January, for each of the years 1982, 1985, 2007, and 2012. Although this study focused on the autumnal months of October and November, the 5-month run span allows for proper model start up. The physics options used for the model runs include: RRTM longwave radiation, Goddard shortwave radiation, Monin-Obukhov (Janjic) surface layer, Noah land surface model, Meller-Yamada-Janjic planetary boundary layer, Grell-Freitas ensemble cumulus parameterization, and Goddard microphysics. Fractional sea ice is turned on, allowing for sea ice concentration to vary in the model. Physics options were chosen following the reference of Seefeldt et al. (2012), and the model's namelist.input file is included as an appendix. Snowfall is calculated by applying a 15 to 1 snowfall ratio to model output non-convective liquid equivalent snowfall. Keeping the snow ratio constant for all the cases will allow model output snowfall to be a direct product of snow liquid equivalent precipitation.

3.3 Case study analysis

Each cyclone from the reduced sea ice extent years is compared with every cyclone from the normal sea ice extent years, with cyclones identified using the WRF model driven by Era-Interim reanalysis data. Cyclones are paired if they occur within the same geographic region within the WRF Domain 2. The date of cyclone occurrence, surface pressure, sea ice extent, moisture source, and 500 hPa height patterns are then analyzed for each cyclone to determine which pairs are suitable for further analysis (Table 3.1). An ideal cyclone pair will: be located over coastal locations where the sea ice extent

differs between the two dates, possess minimum sea level pressure differences of ≤ 10 hPa during the time of track overlap, draw moisture from the Arctic Ocean (including Barents, Kara, Norwegian, and/or Greenland Sea), and have a similar 500 hPa height pattern. Cyclone pairs that fulfill all four of the requirements are selected for further analysis, and act as the cases used in this study. Three cases are chosen for analysis, and are highlighted in Table 3.1, with their tracks shown in Figure 3.2

The cyclones are matched on the dates when they are positioned closest to each other (initial date). The life span of the cyclones vary, so a two-day period is selected from each cyclone's life span for analysis to maintain a consistent sample time period for each cyclone (Figure 3.3 and Table 3.2). The 2-day period is selected starting with the initial date used the match the cyclones, and then adding the day before or after the initial date to produce the 2-day sample period. Determining whether a day is added before or after the initial date is dependent on the stage of the cyclone's life, with the goal to capture each cyclone during the strongest stage of its life cycle.

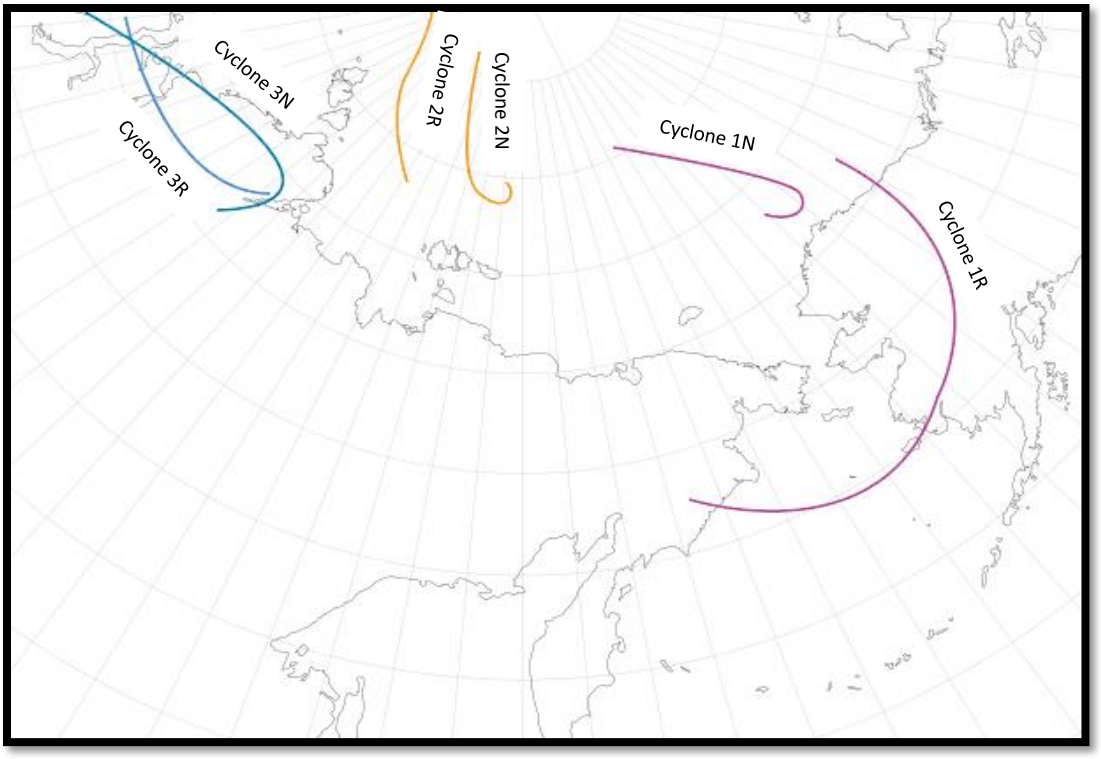

Figure 3.2.

Cyclone tracks (path of minimum mean sea level pressure) for Case 1: (purple), Case 2 (orange), and Case 3 (blue)

Table 3.1. List of paired cyclones considered for study

Potential cyclone pairs		Selected case studies are highlighted
Reduced sea ice cyclones	**Normal sea ice cyclones**	**Colors correspond to tracks in Figure 3.2**
10/28-11/2 2012	10/21-10/25 1982	**Case 1**
10/28-11/2 2012	11/5-11/7 1985	
10/28-11/2 2012	10/21-10/25 1985	
10/28-11/2 2012	11/8-11/10 1982	
11/18-11/22 2012	11/16-11/18 1985	
10/24-10/28 2007	10/21-10/25 1985	
10/24-10/28 2007	11/5-11/7 1985	
10/24-10/28 2007	10/21-10/25 1982	
11/8-11/10 2007	11/5-11/7 1985	
11/8-11/10 2007	10/21-10/25 1982	
11/8-11/10 2007	10/21-10/25 1985	
11/8-11/10 2007	11/16-11/18 1985	
10/3-10/7 2007	10/8-10/16 1985	**Case 2**
10/3-10/7 2007	10/24-10/28 2007	
10/24-10/26 2012	10/16-10/21 1982	
10/26-11/2 2007	10/19-10/25 1985	**Case 3**
10/26-11/2 2007	10/16-10/21 1982	
10/26-11/2 2007	11/26-11/30 1982	
11/1-11/3 2007	11/9-11/12 1985	

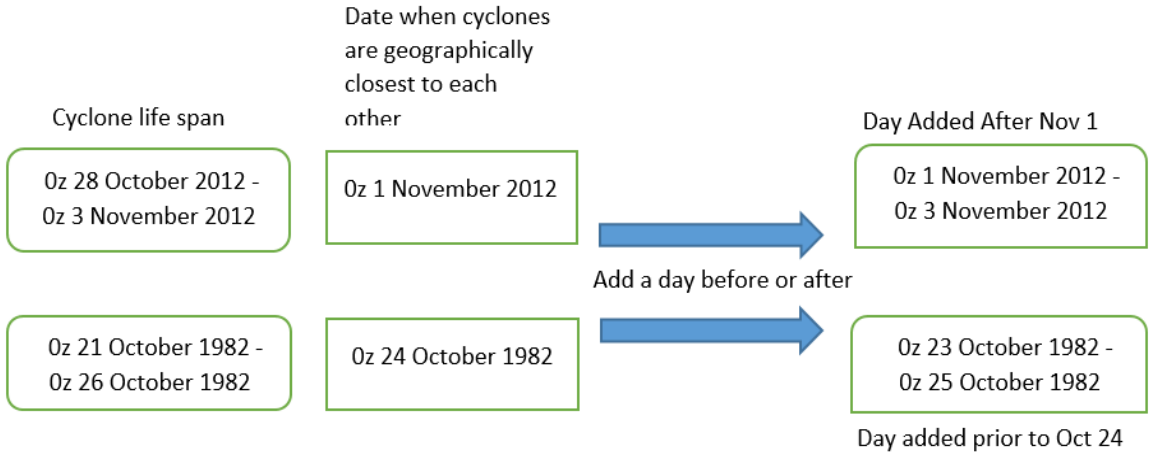

Figure 3.3.

Method for choosing 2-day cyclone sample periods, using Case 3 as an example

Table 3.2. Selected cyclone 2-day sample periods

Cyclone pairs for case study analysis	**Date when cyclone pairs are geographically nearest each other (initial date)**	**2-day sample periods**
Cyclone 1R:10/26-11/2 2007	1R: 00 UTC 1 November 2007	1R: 00 UTC 31 October 2007-00 UTC 2 November 2007
Cyclone 1N:10/19-10/25 1985	1N: 00 UTC 21 October 1985	1N: 00 UTC 21 October 1985-00 UTC 23 October 1985
Cyclone 2R: 10/3-10/7 2007	2R: 00 UTC 6 October 2007	2R: 00 UTC 5 October 2007-00 UTC 7 October 2007
Cyclone 2N: 10/8-10/16 1985	2N: 00 UTC 9 October 1985	2N: 00 UTC 9 October 1985-00 UTC 11 October 1985
Cyclone 3R: 10/28-11/2 2012	3R: 00 UTC 1 November 2012	3R: 00 UTC 1 November2012-00 UTC 3 November 2012
Cyclone 3N: 10/21-10/25 1982	3N: 00 UTC 24 October 1982	3N: 00 UTC 23 October 1982-00 UTC 24 October 1982

The variables analyzed in the case study analysis include sea level pressure with surface winds, HYSPLIT parcel 72-hour back-trajectory history, total column precipitable water, 500 hPa heights, total snowfall over the selected 2-day period, and sea ice extent. An analysis of 2-day snowfall differences is also produced for each case study analysis. This increase in snowfall should occur over or downwind of regions where sea ice is anomalously low to support the hypothesis, as the snowfall increase would then be a result of the open waters over the Arctic Ocean to support the hypothesis.

3.4 Parcel back-trajectories

To determine the moisture source for the cyclones in each study case, parcel back-trajectories are produced using the downloadable version of the HYSPLIT trajectory model (Stein et al. 2015, Rolph et al. 2017). The HYSPLIT model is used to run a 5 by 5 matrix of back-trajectories, extending back 72 hours from the initialization time. The sampled parcels are separated at initialization by 2 degrees latitude and; 10 degrees longitude for cyclones 3N, 2R, and 1N, 5 degrees latitude for cyclones 2N and 3R, and 4 degrees longitude for cyclone 1R. The matrices are centered over the cyclone centers, with the varied longitudinal separation of parcel initialization points used to account for the differing latitudes at which the cyclones traverse. The HYSPLIT model is run using the ERA-Interim reanalysis dataset. Vertical motion occurs in the back-trajectories utilizing the modeled vertical velocity from the ERA-Interim reanalysis dataset, with the parcels starting at 10 m above the surface (ground level or terrain height).

3.5 Monthly snowfall analysis

The analyses of monthly snowfall and snow depth are produced from the examination of WRF model output. The monthly snowfall analysis investigates the monthly total snowfall accumulation for October and November of 1982, 1985, 2007, and 2012. Snow depth is analyzed on 31 October and 30 November of 1982, 1985, 2007, and 2012.

Monthly snowfall and snow depth differences between the years with normal sea ice extent and reduced sea ice extent are also produced. Average monthly snowfalls are computed by averaging the monthly snowfall occurring in the normal sea ice extent years (1982 and 1985), and separately averaging the monthly snowfalls occurring in the reduced sea ice extent years (2007 and 2012). The average monthly snowfall for the normal sea ice extent years is subtracted from the average monthly snowfall for the reduced sea ice extent years to produce a snowfall difference. Snowfall differences are computed separately for the months of October and November. Average Snow depths are computed by taking the snow depth average of the normal sea ice extent years and, separately, the snow depth average of the reduced sea ice extent years. The snow depth average for the normal sea ice extent years is subtracted from the snow depth average for the reduced sea ice extent years to produce a snow depth difference. Snow depth differences are computed for 31 October and 30 November of the four studies years.

CHAPTER 4: RESULTS

4.1 Monthly snowfall analysis

The examination of October and November monthly total snowfall (Figure 4.1) and snow depth (Figure 4.2) for 1982, 1985, 2007, and 2012 will primarily focus on snowfall occurring over the Arctic Ocean and over high-latitude continental regions near the Arctic coast. Less emphasis will be put on locations southward away from the Arctic coastline. For this reason, southeastern Siberia and southwestern Alaska will be given less attention, as most of the snowfall that occurs there is due to storm tracks originating over the northwestern Pacific Ocean. Monthly snowfall and snow depth data are derived from WRF simulations forced by the Era-Interim reanalysis dataset. Applying a constant snow ratio to model output liquid-equivalent snow precipitation means that snowfall totals will be counted over both land and oceanic regions. Although snow cannot accumulate over liquid water, snowfall that occurs over open water will be analyzed in the monthly snowfall analysis, while the snow depth analysis will leave open water devoid of snow. The model will allow snow depth to exist over patchy sea ice extents, including regions just outside the 15% sea ice isopleth used to define sea ice extent. Snow depth will be reported when depth reaches or exceeds 0.1 cm.

October of 1982 and 1985, the normal sea ice extent years, have their greatest monthly snow totals over continental regions and along the Arctic coast, with monthly snowfall declining toward the central Arctic Ocean (Figure 4.1). October monthly snowfall along the Arctic coastline generally exceeds 20 cm, while snowfall over the central Arctic Ocean totals less than 20 cm. October of 2007 and 2012, the reduced sea ice extent

years, experience higher monthly snowfall amounts across the Arctic Ocean relative to the normal sea ice extent years. Snowfall exceeds 20 cm in all locations in the domain, expect for eastern Siberia in October 2007. Snow amounts surpass 50 cm across western Siberia and the Kara Sea in October 2007, and over the East Siberian Sea and northern Alaska in October 2012. Monthly snowfall totals are less in November compared to October for most studied years, except for 1985, where the central Arctic Ocean is shown to receive higher snowfall, up to 60 cm, compared to the less than 20 cm that is produced by the model during the month of October. The decrease in snowfall from October to November is expected, as less moisture is available with greater sea ice extent and a lower temperature in the region.

There appears to be a relationship between sea ice extent and snowfall occurring over the Arctic Ocean in October. The average monthly snowfall in the reduced sea ice extent years, with more open water, is up to 30 cm greater than the average monthly snowfall for the normal sea ice extent years over the central Arctic Ocean in October (Figure 4.3). In November, average monthly snowfall is greater for the normal sea ice extent years than the reduced sea ice extent years by about 20-30 cm across the central Arctic Ocean, northward of the East Siberian Sea, while average monthly snowfall is greater in the reduced sea ice extent years by about 10-20 cm over the region northward of the Kara Sea (Figure 4.4). Though a relationship looks to exist, a greater sea ice extent will not always mean lower snowfall over the Arctic Ocean, as moisture transport from lower latitudes can occur. It is likely the case that a greater chance for above average snowfall exists in anomalously low sea ice extent environments, while the odds of below average snowfall increases when the sea ice is close to or above average. It is more difficult to

discern a relationship between the sea ice extent and snowfall occurring over continental locations. For the continental regions, the differences in average monthly snowfall between the reduced and normal sea ice extent years are noisy, especially farther inland. Further studies may be needed to investigate the relationship between monthly snowfall and autumnal Arctic sea ice extent.

In both October (Figure 4.5) and November (Figure 4.6), less snow depth is displayed in the reduced sea ice extent years than the normal sea ice extent years across the southern Arctic Ocean. This is largely due to the differences in sea ice extent, as autumn snow depth is zero across the ice-free southern Arctic Ocean in the reduced sea ice extent years (Figure 3.1), preventing snow from accumulating. Snow depth accumulates up to 20 cm across the regions of sparse sea ice cover across the southern Arctic Ocean in October 2007 and 2012, though much of this region is free of ice and snow (Figure 4.2). In the normal sea ice extent years, modeled October snow depth exceeds 10 cm across the entire Arctic Ocean basin, excluding the Kara Sea in 1985 where snow depth is lower. October snow depth reaches up to 30-40 cm in some regions of the southern Arctic Ocean in the normal sea ice extent years. In both October and November, average snow depth is generally 10-30 cm greater in the normal sea ice extent years than the reduced sea ice extent years across the southern Arctic Ocean (Figure 4.5 and 4.6), mostly due to the lack of autumnal sea ice coverage in the reduced sea ice extent years. As is the case with the monthly snowfall, snow depth over the continental regions is noisy for both October and November. For both months, average snow depth is approximately 10-20 cm greater in western Siberia for the reduced sea ice extent years than the normal sea ice extent years (Figure 4.5 and 4.6). Snow depth is 10-20 cm less over the central and

eastern Siberia coastlines in the reduced sea ice extent years than the normal sea ice extent years, partially due to a less active storm track across the region in October 2007, which may or may not be related to the reduced sea ice extent.

It can be inferred from the data that after most of the Arctic Ocean has become iced over by the end of November, the snow depth on top of the seasonal sea ice in the reduced sea ice extent years lags the snow depth in the normal sea ice extent years, as snow is not able to accumulate until there is ice cover. Areas where multi-year ice exists will accumulate snow through the entire autumn season. When investigating (and isolating) the impact of sea ice decline on snow depth over the existing ice cover, only snow depth over multi-year ice can be considered, as this ice cover will accumulate snow throughout the entire autumn season. Interestingly, the small region of multi-year ice near the North Pole in the reduced sea ice extent years observe greater snowfall (Figures 4.3 and 4.4) and snow depth (Figures 4.5 and 4.6) than the same region in the normal sea ice extent years. This may indicate that snow depth increases in the reduced sea ice extent years over the remaining multi-year ice, which could be a result of increasing snowfall from a decrease in sea ice extent.

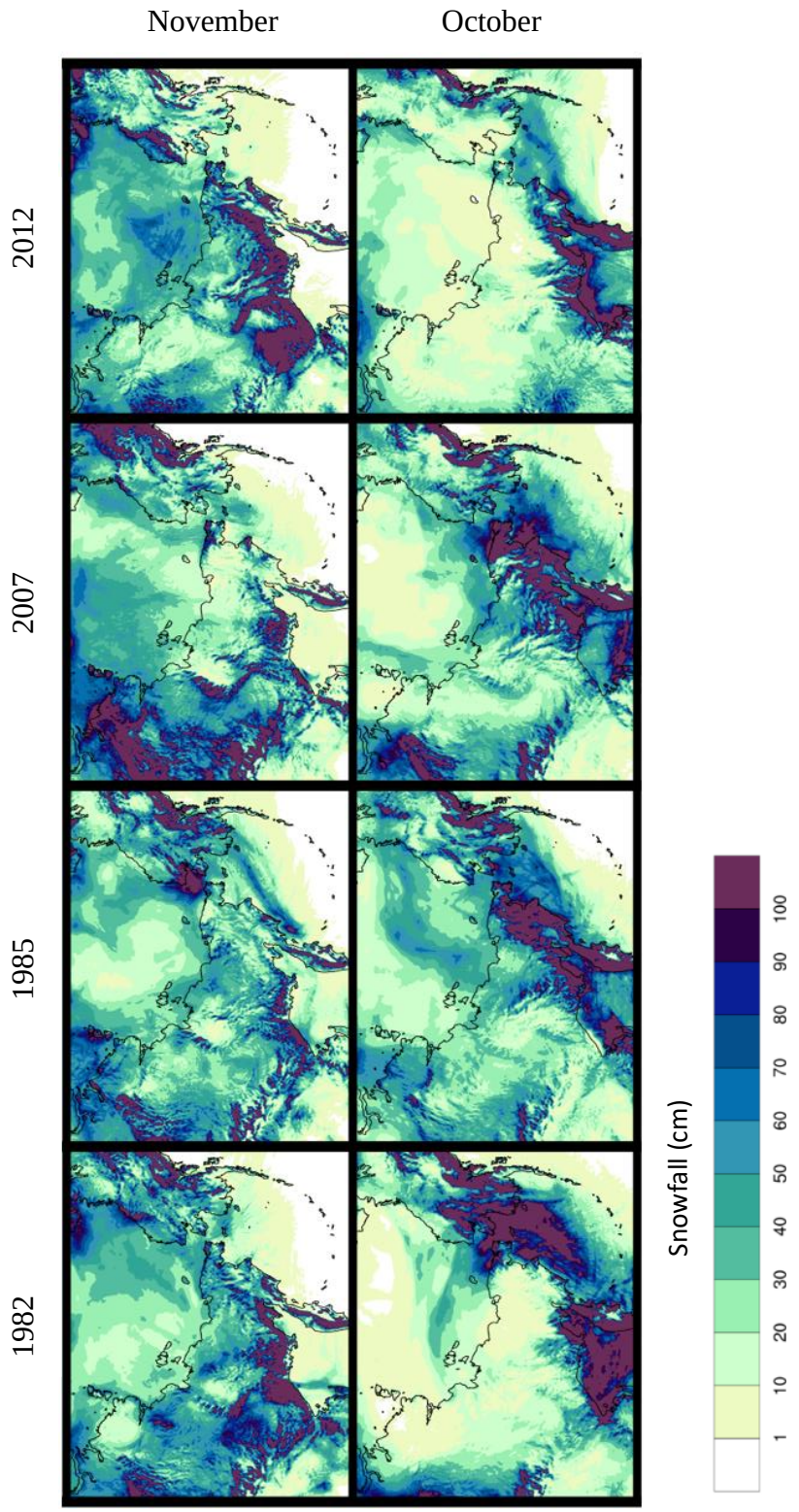

Figure 4.1.

Monthly total snowfall (cm) for October and November of 1982, 1985, 2007, and 2012

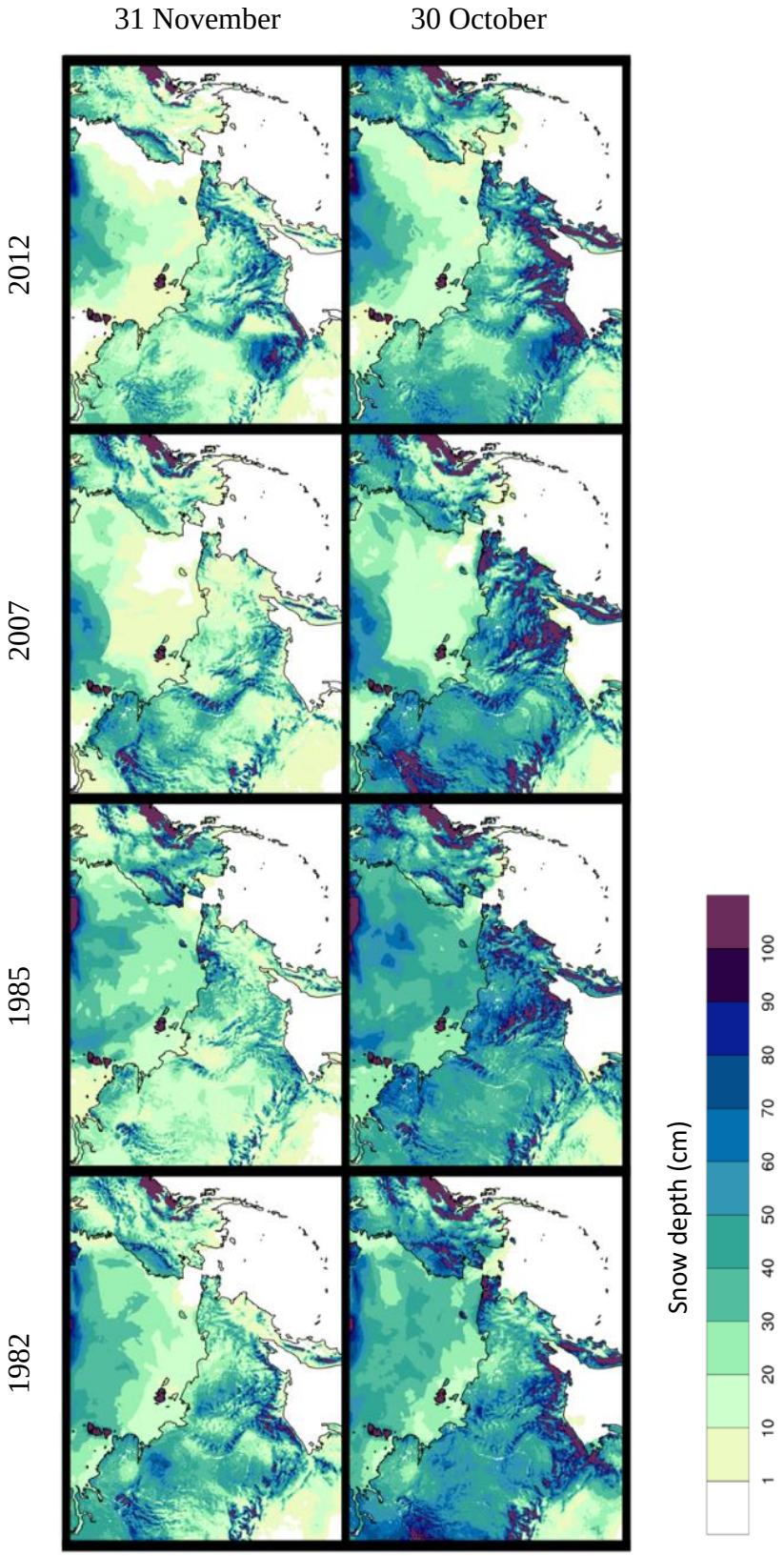

Figure 4.2.

Snow depth (cm) for 31 October and 30 November of 1982, 1985, 2007, and 2012

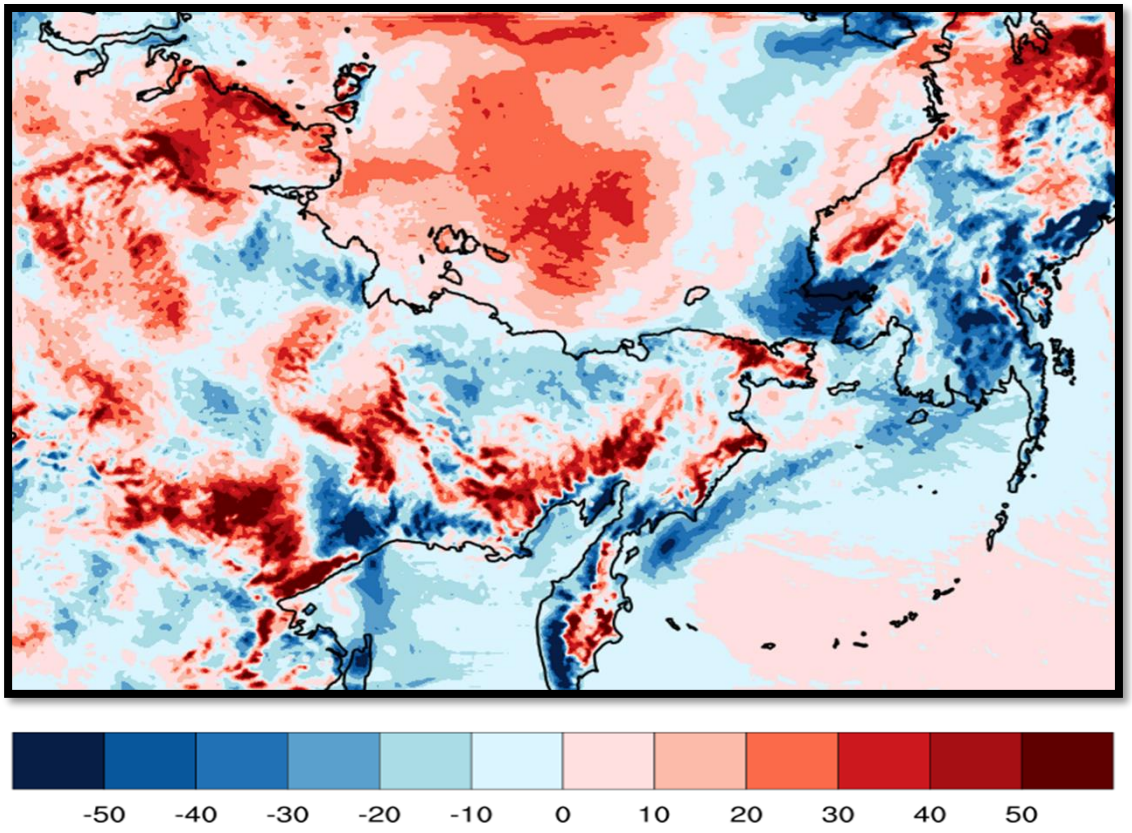

Figure 4.3.

Difference in monthly total snowfall (cm) between the reduced and normal sea ice extent years in October (reduced ice years – normal ice years)

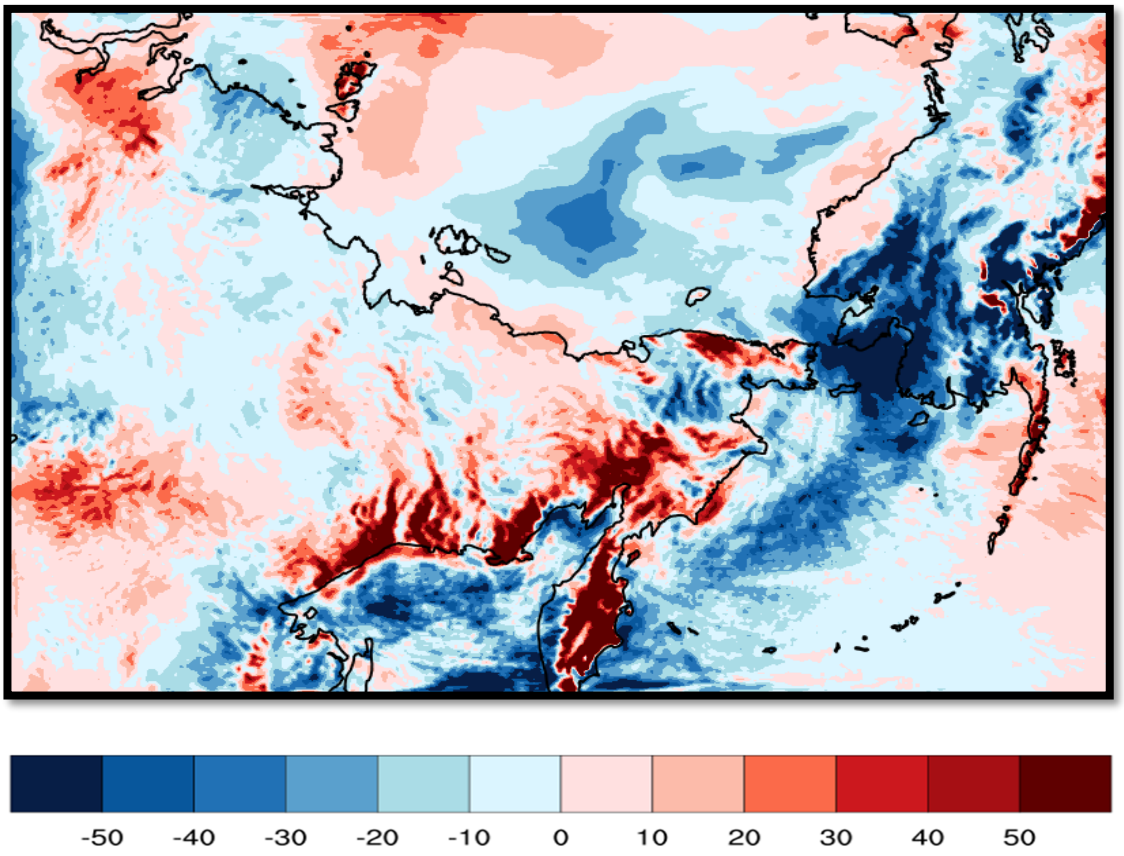

Figure 4.4.

Difference in monthly total snowfall (cm) between the reduced and normal sea ice extent years in November (reduced ice years – normal ice years)

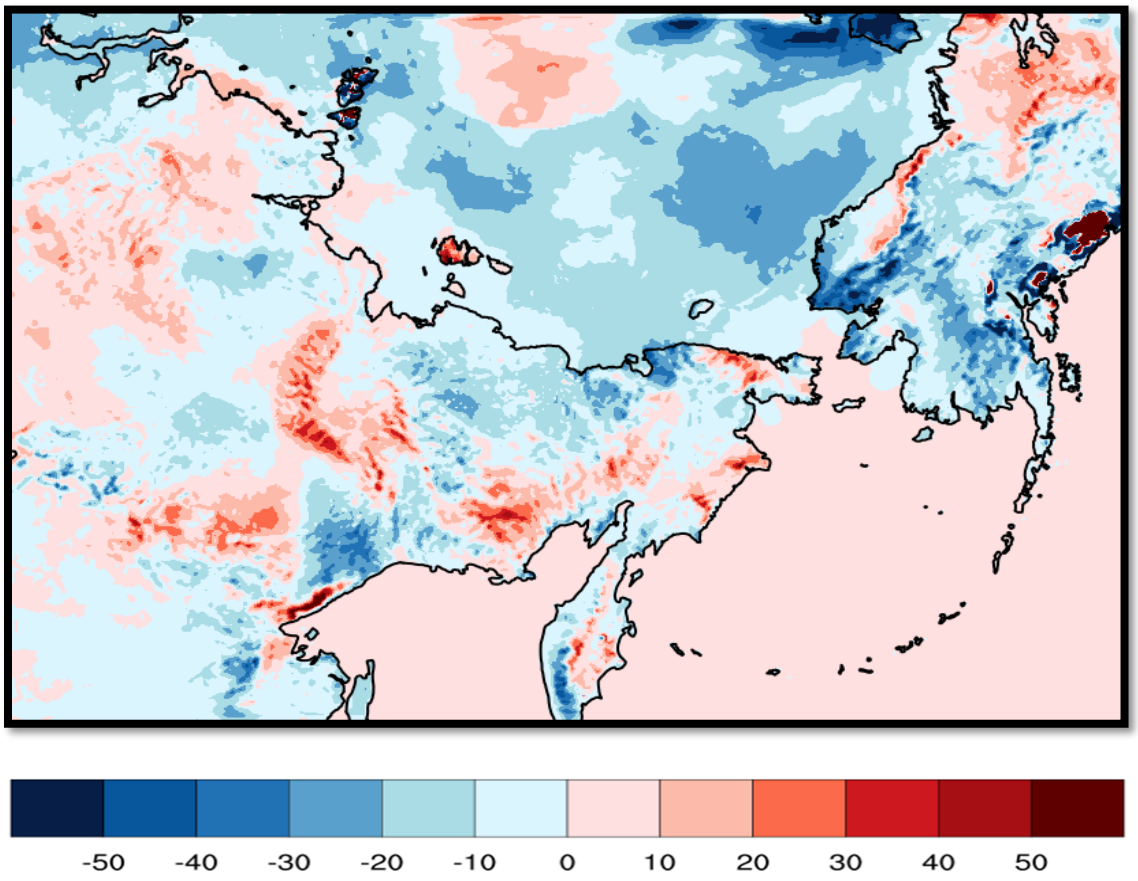

Figure 4.5.

Difference in snow depth (cm) between the reduced and normal sea ice years at 00 UTC 31 October (reduced ice years - normal ice years)

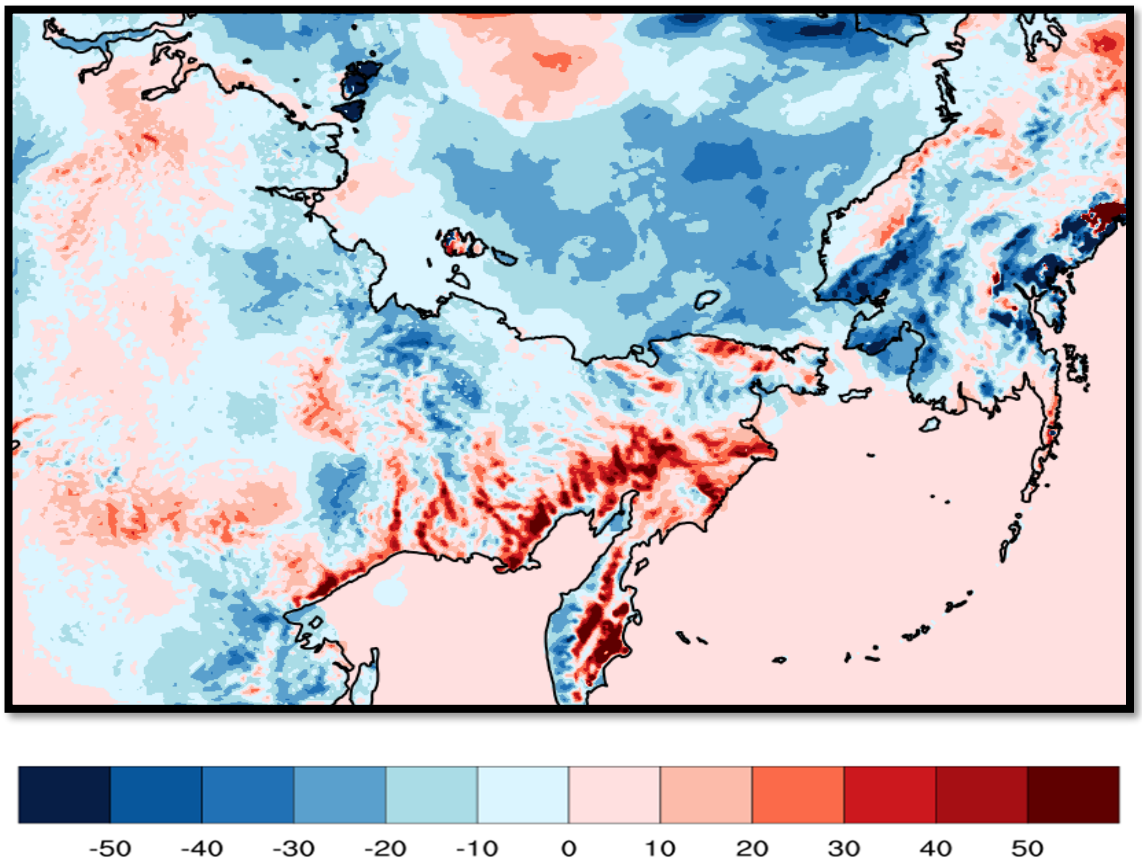

Figure 4.6.

Difference in snow depth (cm) between the reduced and normal sea ice years on 00 UTC 30 November (reduced ice years - normal ice years)

4.2 Case study analysis

The goal of the case study analysis is to identify increases in snowfall due to a decrease in sea ice extent between pairs of cyclones with similar characteristics and paths. These snowfall increases should coincide geographically with decreasing sea ice extent, where augmented sensible and latent heat fluxes are expected to occur.

4.2.1 Case 1

The low-pressure center for Cyclone 1R is located over the Brooks Range of Alaska, with the northern portion of the cyclone over an environment with reduced Arctic sea ice extent (Figure 4.7 A and E). Cyclone 1R has a minimum mean sea level pressure (MSLP) of approximately 971 hPa. The low-pressure center for Cyclone 1N is located slightly northward of the Arctic coast of Alaska and occurs over an environment with normal Arctic sea ice extent relative to Cyclone 1R (Figure 4.7 F and J). Cyclone 1N has a minimum MSLP of approximately 967 hPa. The HYSPLIT back-trajectory analyses show that each cyclone draws most of its air from over the Arctic Ocean, with the parcels in both cyclones remaining in the lower atmosphere below 800 hPa (Figure 4.8 A and B). Analysis of precipitable water (PW) shows that Cyclone 1R contains more moisture, with PW exceeding 14 mm on the eastern end of the storm and PW of 6-8 mm on the western side (Figure 4.7 B). Cyclone 1N has PW of only up to 10 mm on the eastern end of the cyclone, with PW dropping below 2 mm on the western end of the storm (Figure 4.7 G). Moisture should be higher when sea ice extent is reduced (Liua et al. 2012), so greater PW within Cyclone 1R is expected. The 500 hPa heights have some differences between the two cyclones, with Cyclone 1N possessing a deeper mid-level low than Cyclone 1R. A closed mid-level low is centered over the Chukchi Sea for Cyclone 1N, with heights

dropping below 4740 gpm (Figure 4.7 H). A closed low is also associated with Cyclone 1R, centered over Central Alaska, with minimum heights around 4980 gpm (Figure 4.7 C).

Cyclone 1R produces a uniform swath of snow along and offshore the Arctic coast of Alaska down to the Bering Strait (Figure 4.7 D). Areas in the Chukchi Sea and western Alaska Arctic coast display snowfall amounts of 7-15 cm, while the eastern Alaska and Yukon Arctic coasts have slightly higher snowfall totals of 10-20 cm. Most of the snowfall in this swath is produced offshore over the Arctic Ocean. Snowfall in Cyclone 1N occurs in two regions (Figure 4.7 I). The first is over the Chukchi Sea, where snowfall amounts of 10-15 cm are depicted by the model over the open waters, with amounts peaking over 30 cm along the coastal highlands of Alaska. Snowfall in this region penetrates inland into northeastern Alaska. A second region has a swath of snow well off the coast of Alaska and the Yukon Territory, where snowfall amounts of 7-10 cm are produced.

Case 1 provides support of the hypothesis, as Cyclone 1R generally produces greater snowfall than Cyclone 1N, even though the surface and mid-level low-pressures are weaker in Cyclone 1R than in Cyclone 1N. The Alaskan coastline receives up to 15 cm more snowfall in Cyclone 1R than in Cyclone 1N (Figure 4.9). Though much of these differences occur offshore, the northernmost region of Alaska, near Barrow, experiences greater snowfall. The Arctic Ocean is ice-free for several hundred kilometers offshore the Alaskan coastline in late October 2007 (Figure 4.7 E). This is the region that experiences greater snowfall in Cyclone 1R (Figure 4.7 D), supporting the hypothesis that more open water will generate greater snowfall. Sea ice coverage in late October 1985 exists along

the northern coast of Alaska (Figure 4.7 J), with open water found only from the Chukchi Sea southward. Snowfall is greater in Cyclone 1N than in Cyclone 1R by up to 15 cm for a smaller region in the Chukchi Sea and northwestern Alaska (Figure 4.9), where the waters are free of ice in late October 1985 (Figure 4.7 J). PW (Figures 4.7 B and G) tends to be higher over the open waters of the Arctic where the greatest snowfall is occurring in each cyclone. PW reaches 6-8 mm off the coast of Alaska compared to less than 4 mm outside of the main snow swath in Cyclone 1R (Figure 4.7 B). PW in Cyclone 1N is also greater over the Chukchi Sea, at 2-4 mm compared to less than 2 mm over sea ice northward of Cyclone 1N (Figure 4.7 G).

The increases in snowfall and precipitable water appear to be occurring locally near and adjacent to the regions of open water in Case 1. It can be interpreted that reduced sea ice will enhance snowfall along the Arctic coast, with lesser impacts on snowfall occurring farther inland. Snowfall that occurs over oceanic regions will not impact snow depth, which is the case for a portion of the snowfall occurring over the open Arctic waters. Snowfall increases over land near the Arctic coastline in Case 1, as well as over ice-covered regions of the Arctic Ocean, likely leading to an increase in snow depth in these regions.

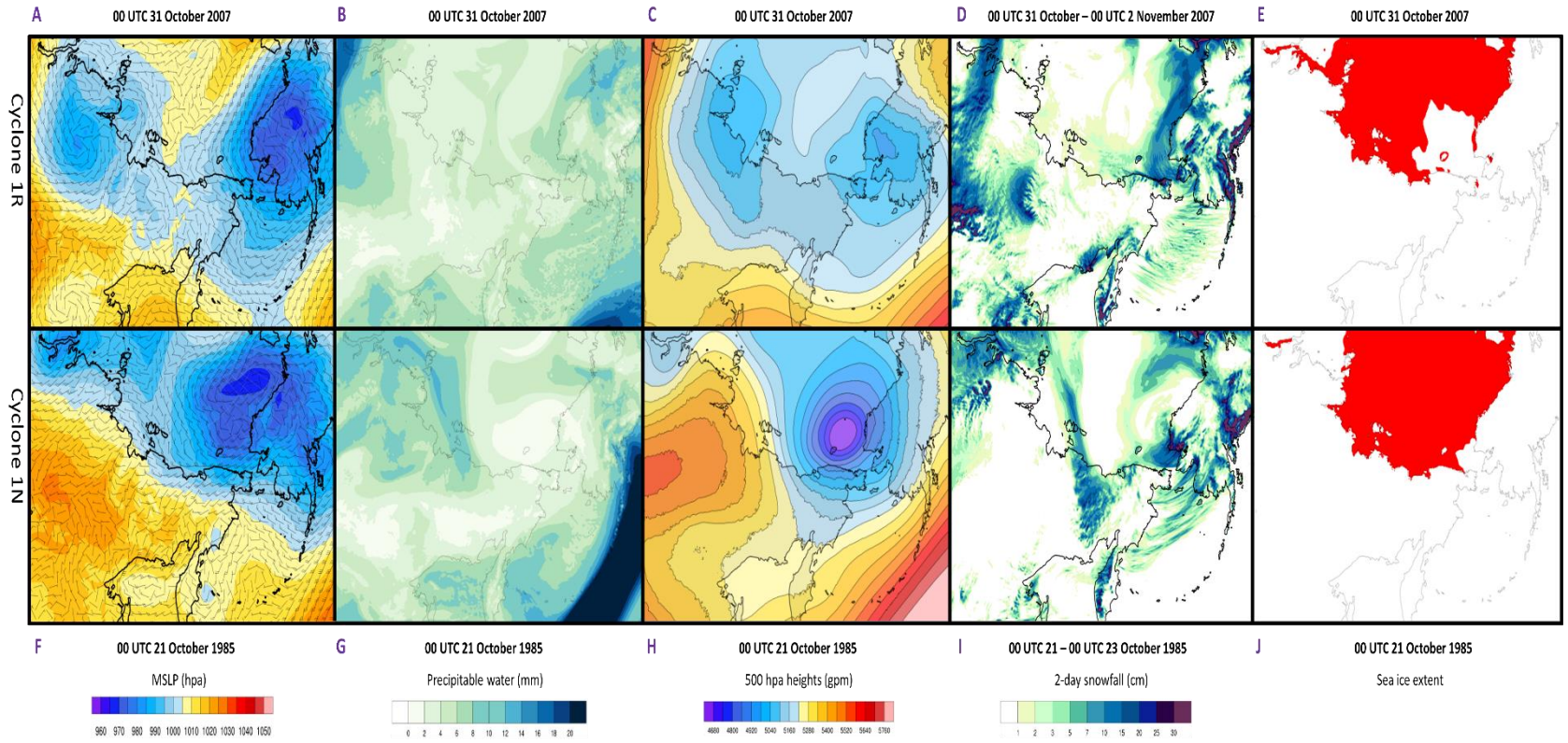

Figure 4.7.
Case study 1, for cyclones occurring on 00 UTC 31 October 2007 – 00 UTC 2 November 2007 and 00 UTC 21 October 1985 – 00 UTC 23 October 1985. MSLP/wind vectors (A and F), precipitable water (B and G), 500 hpa heights (C and H), total accumulated snowfall (D and I), and sea ice extent (E and J) are displayed

A

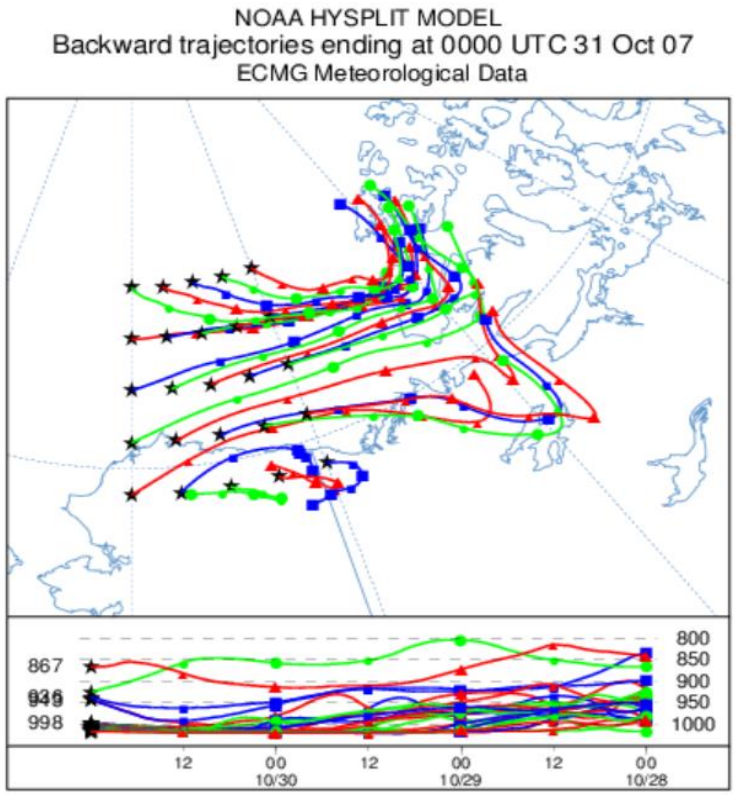

B

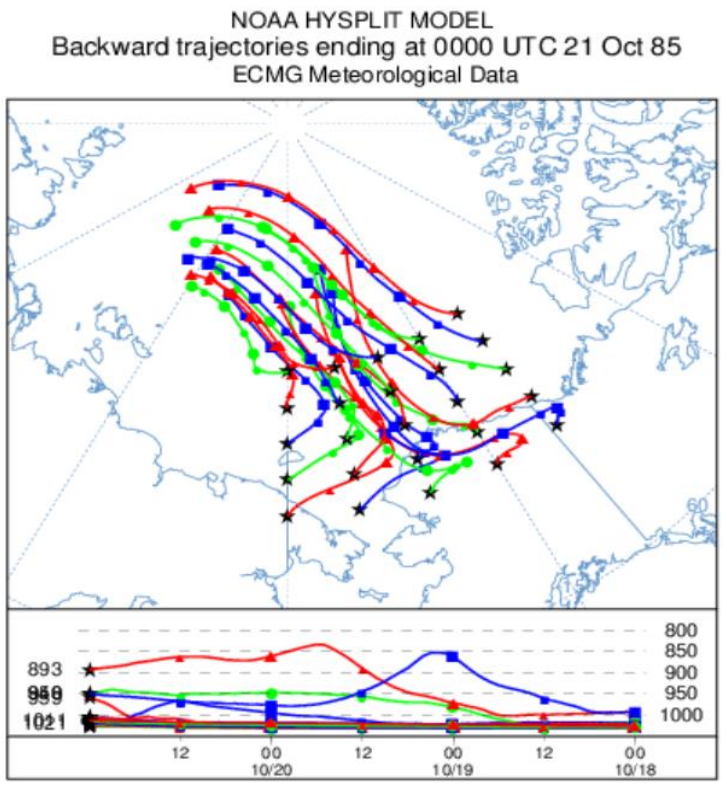

Figure 4.8.

HYSPLIT 72 hour back-trajectory analysis for Cyclone 1R (A) and Cyclone 1N (B), the varied colors of the HYSPLIT back-trajectories hold no importance other than allowing for an easier distinction between the parcel trajectories

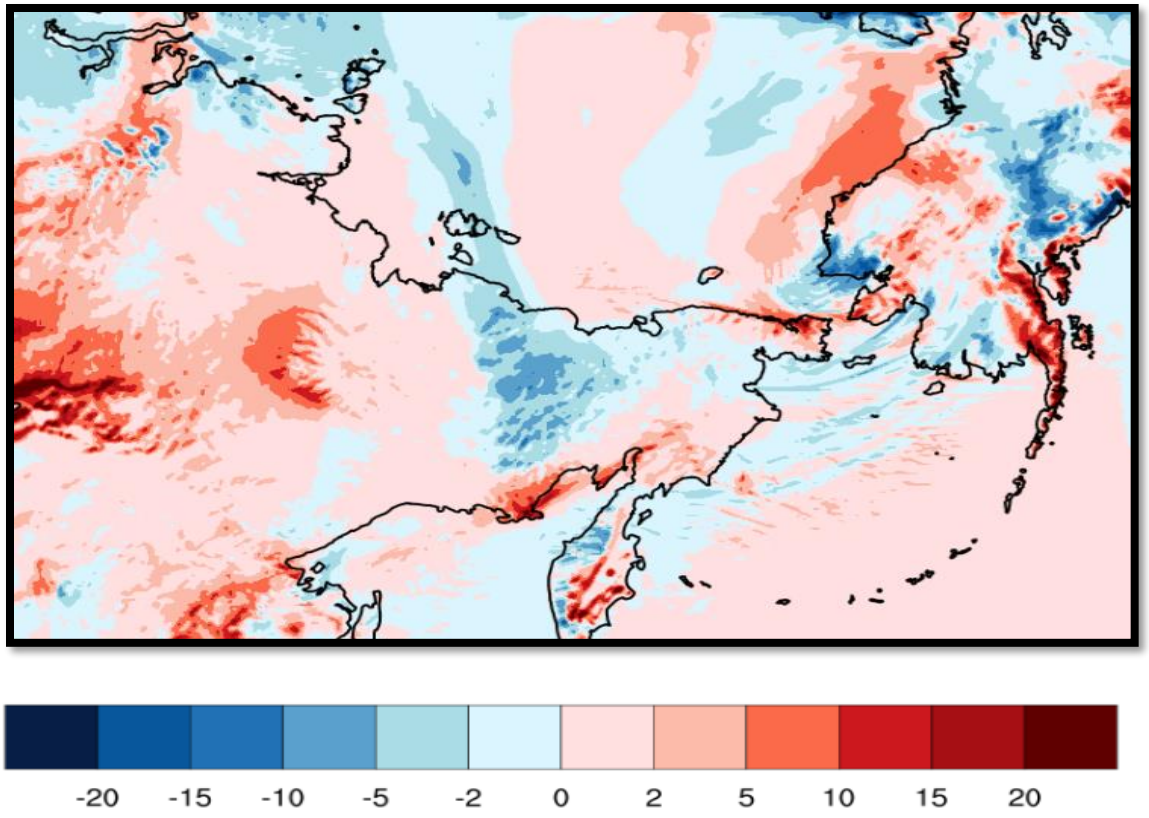

Figure 4.9.

Difference in snowfall (cm) occurring between cyclone 1R and cyclone 1N (cyclone 1R – cyclone 1N)

4.2.2 **Case 2**

Case 2 consists of a pair of cyclones off the Arctic coast of Siberia. Cyclone 2R is centered between the Laptev and Kara Seas, and exists over an environment with reduced Arctic sea ice extent (Figure 4.10 A and E). Cyclone 2R has a minimum MSLP of approximately 975 hPa. Cyclone 2N is centered over the Arctic Ocean, slightly north of the Laptev Sea, and exists over an environment with greater Arctic sea ice extent relative to Cyclone 2R (Figure 4.10 F and J). Cyclone 2N has a minimum MSLP of 985 hPa. The 72-hour HYSPLIT back-trajectory analyses show that both cyclones draw in air from the Arctic Ocean and the Barents/Kara Seas, with modeled parcels tracking through the lower atmosphere below 850 hPa in both cyclones (Figure 4.11 A and B). PW is similar in the two cyclones, though Cyclone 2N has slightly higher moisture on the western side of the storm. PW for Cyclone 2R is around 4-8 mm, with a quasi-uniform distribution of moisture throughout the system (Figure 4.10 B). Cyclone 2N has most of its moisture concentrated on the western side of the storm, with 9-14 mm in the region with maximum PW (Figure 4.10 G). Very low PW of less than 2 mm exists in the eastern side of Cyclone 2N. The 500 hPa analyses show that the troughs associated with the cyclones are of similar strength, though the trough over Cyclone 2N is more compact and centered slightly northward. Minimum 500 hPa heights are 4950 gpm and 4840 gpm for Cyclones 2R and 2N, respectively, and the mid-level low is found nearly stacked on top of the surface low in both cases (Figure 4.10 C and H).

Snowfall totals differ between the cyclone cases. The snowfall field is spatially more extensive in Cyclone 2R than in Cyclone 2N, extending far offshore the Siberian coastline. Over the Arctic Ocean, the highest snowfall totals in Cyclone 2R occur in a

band on the northern end of the cyclone near the North Pole, where 7-15 cm of snowfall is shown (Figure 4.10 D). Regions eastward of the surface low over the ocean display 1-7 cm of snow, with locally higher amounts. Over Siberia, the highest snowfall amounts are directly south of the Kara Sea, where totals of 7-15 cm are produced by the model. Lesser amounts, 1-5 cm, are produced inland, except for locally higher snow totals that are found over mountainous regions. The snowfall associated with Cyclone 2N falls in a more discrete band over the Laptev Sea, southern Kara Sea, and adjacent landmasses (Figure 4.10 I). Snowfall totals of 7-15 cm are common in this region. A secondary weaker region of snowfall also occurs over the central Arctic Ocean eastward of the surface low, where snowfall from 1-10 cm is indicated. The peak snowfall is similar within the two cyclones, though the snowfall in Cyclone 2R covers a much greater geographic area than the snowfall in Cyclone 2N.

Case 2 also supports the hypothesis. The sea ice extent in early October 2012 remains reduced across most of the Eurasian coastline, especially in the region northward of the Chukchi Sea (Figure 4.10 E). A southerly surface wind flow on the eastern side of the cyclone allows for a long fetch over the ice-free regions of the Arctic Ocean. The anomalous deficit of sea ice extent allows for an increase in heat and moisture fluxes, likely decreasing low-level stability and fostering greater snowfall eastward of Cyclone 2R (Figure 4.10 D). Snowfall is greater by 1-5 cm across the central Arctic Ocean northward of the East Siberian Sea between Cyclone 2R and 2N (Figure 4.12), with snowfall increasing by about 5-10 cm closer to the North Pole. The occurrence of enhanced snowfall up to the North Pole could mean that some of the moisture from the ice-free regions is advecting over ice-covered regions northward of Cyclone 2R, a

difference from Case 1, where snowfall enhancement only occurs near the ice-free waters of the Arctic Ocean.

Cyclone 2R is deeper than Cyclone 2N by about 10 hPa (Figure 4.10 A and F), and covers a larger geographic area than Cyclone 2N. Snowfall is also greater over the continental regions of Cyclone 2R compared to Cyclone 2N, even in regions without a direct fetch from the Ocean (Figure 4.12). These factors may signal that there are variables other than reduced sea ice extent, such as an increase in forcing for ascent, that are also contributing to the greater snowfall observed in Cyclones 2R than cyclone 2N. This is not to say that reduced sea ice extent does not have an impact on the greater snowfall found in Cyclone 2R, however it may be that a lesser sea ice extent relative to cyclone 2N is enhancing the snowfall already produced in Cyclone 2R, particularly on the eastern and northern sides of the cyclone.

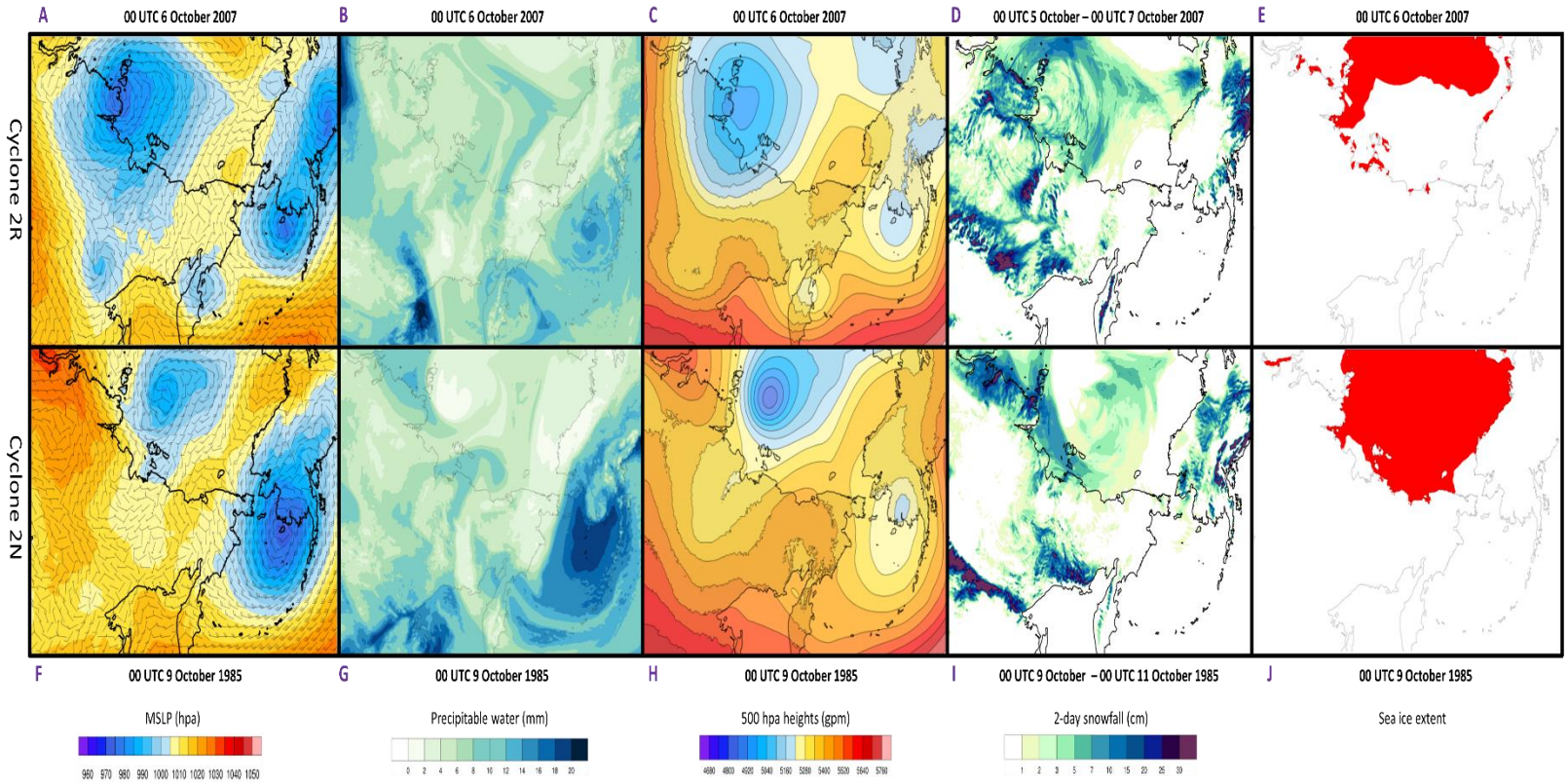

Figure 4.10.
Case study 2, for cyclones occurring on 00 UTC 5 October – 00 UTC 7 October 2007 and 00 UTC 9 October 1985 – 00 UTC 11 October 1985. MSLP/wind vectors (A and F), precipitable water (B and G), 500 hpa heights (C and H), total accumulated snowfall (D and I), and sea ice extent (E and J) are displayed

A

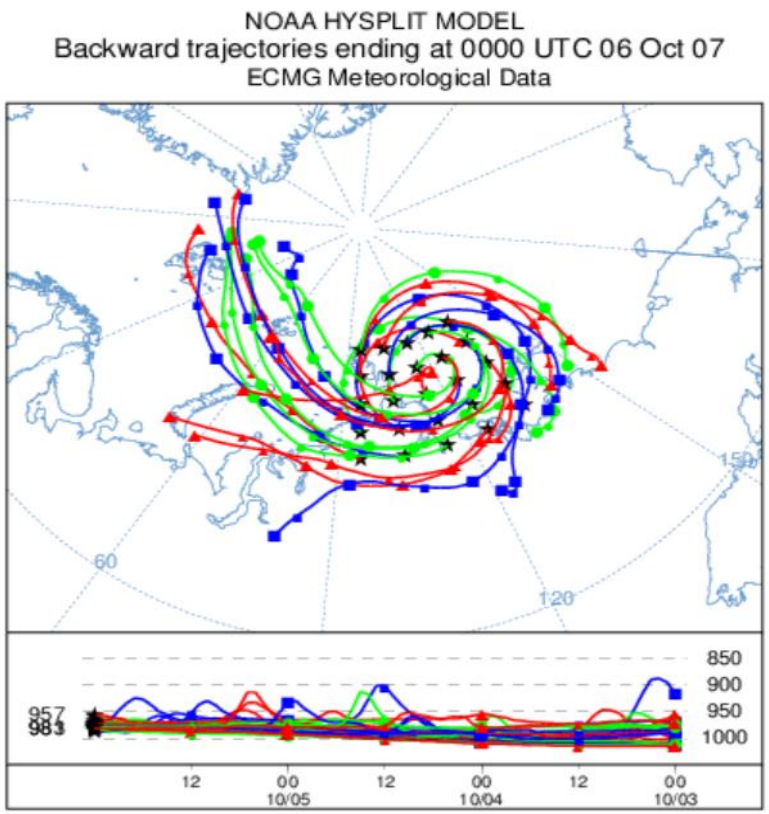

B

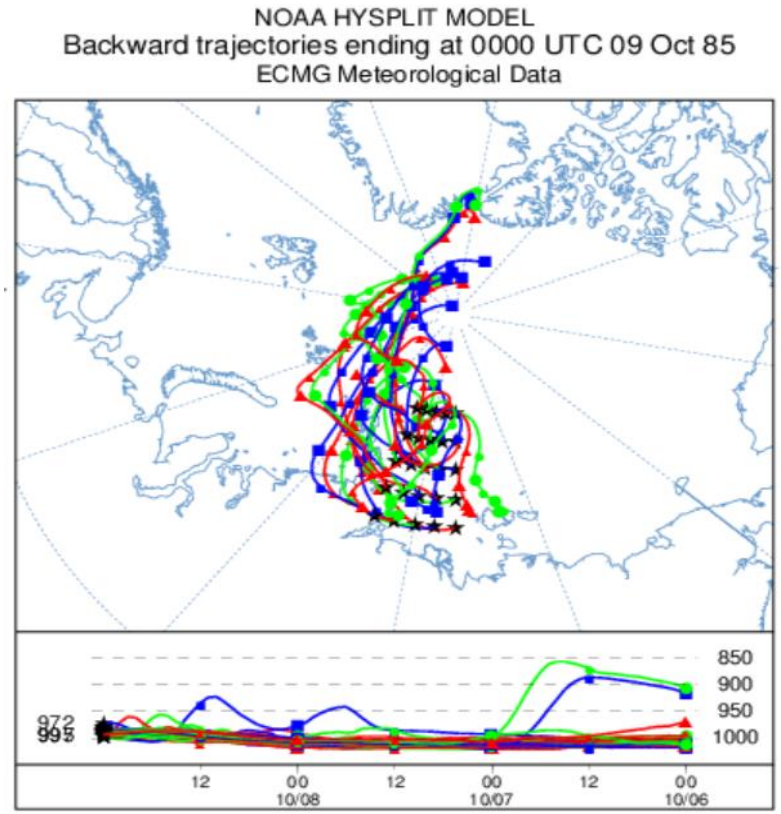

Figure 4.11.

HYSPLIT 72 hour back-trajectory analysis for Cyclone 2R (A) and Cyclone 2N (B), the varied colors of the HYSPLIT back-trajectories hold no importance other than allowing for an easier distinction between the parcel trajectories

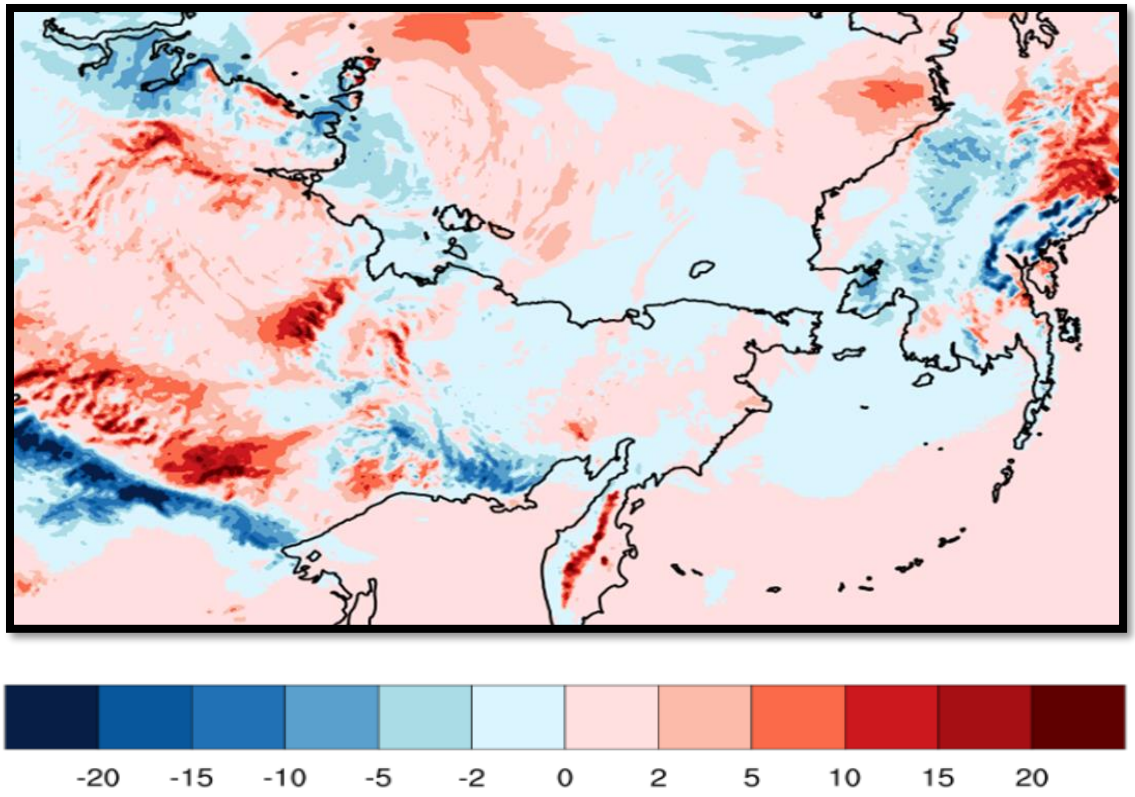

Figure 4.12.

Difference in snowfall (cm) occurring between cyclone 2R and cyclone 2N (cyclone 2R – cyclone 2N)

4.2.3 **Case 3**

Case 3 focuses on a cyclone pair on the western side of the domain, over northern Eurasia. Cyclone 3R is centered over north-central Siberia, with the northern portion of the cyclone over an environment with reduced Arctic sea ice extent (Figure 4.13 A and E). Cyclone 3R has a minimum MSLP of 991 hPa. Cyclone 3N is found along the coastline of north-central Siberia, though farther northward near the western Laptev Sea with the northern portion of the cyclone over an environment with normal Arctic sea ice extent relative to cyclone 3R (Figure 4.13 F and J). Cyclone 3N has a minimum MSLP of 994 hPa. Both cyclones produce onshore winds on the northwestern side of the storm, though Cyclone 3N creates offshore winds on the eastern side of the system as opposed to a weak onshore flow observed on the eastern side of Cyclone 3R. The HYSPLIT back-trajectory analysis shows that air originating over the Laptev and Kara Seas is drawn into Cyclone 3N and the far northern end of Cyclone 3R, with parcels remaining below 800 hPa (Figures 4.14 A and B). Moisture is higher with Cyclone 3R, with PW of 8-12 mm found within the vicinity of the system (Figure 4.13 B). Cyclone 3N has lesser PW of 4-8 mm within the storm (Figure 4.13 G). The 500 hPa height patterns for both cyclones are similar, with weak lows existing above each of the cyclones. Cyclone 3R's 500 hPa low is found nearly stacked on top of the surface low with minimum heights of around 5100 gpm (Figure 4.13 C), whereas the 500 hPa low associated with Cyclone 3N is found slightly westward of the surface low, with a height minimum of approximately 5000 gpm (Figure 4.13 H).

Snowfall is higher in Cyclone 3N than in Cyclone 3R. Cyclone 3R develops a region of snowfall on the northern end of the cyclone, with 7-15 cm of snowfall accumulation in

the main swath (Figure 4.13 D). Cyclone 3N has a much larger region of snowfall, extending across the Kara Sea, and southward into central Siberia. Snowfall in this region is generally from 7-15 cm, with a localized region of greater snowfall eastward of Proliv Krasnoy Armii where amounts exceed 15 cm (Figure 4.13 I). Overall, Cyclone 3N has a much larger region with snowfall associated with the system, though the snowfall amounts within the snowfall band are similar to those experienced in Cyclone 3R (Figure 4.13 D and I).

The results from Case 3 do not support nor deny the hypothesis. Cyclone 3N is shown to produce greater snowfall across both north-central Siberia and over the Kara Sea than Cyclone 3R (Figure 4.15), where snowfall is approximately 5-10 cm greater in Cyclone 3N than in Cyclone 3R. Cyclone 3R produces greater snowfall than Cyclone 3N in a region of north-central Siberia by about 2-10 cm, though the region is smaller than the area where snowfall is greater from Cyclone 3R than from Cyclone 3N (Figure 4.15). Both cyclones produce onshore winds on the northwestern side of the cyclone. Cyclone 3R draws air from over a patchy sea ice environment, though much of the air traveling into cyclone 3R originates over land, while Cyclone 3N draws air from an environment with full sea ice coverage (Figure 4.13 E and J). The surface lows are of similar magnitude (Figure 4.13 A and F), and the 500 hPa height pattern shows little difference between the cases (Figure 4.13 C and H).

There are many factors that were not controlled for in this study that could potentially lead to Cyclone 3N producing greater snowfall than Cyclone 3R (Figure 4.15). It is possible that variables such as temperature or forcing for lift have a stronger impact on the snowfall in Case 3 than differences in sea ice extent. It is also possible that Cyclone

3R did not draw enough moisture from the open waters to the north to increase snowfall, possibly a result of poor case selection as the HYSPLIT analysis shows most of the modeled parcels originating over land in Cyclone 3R.

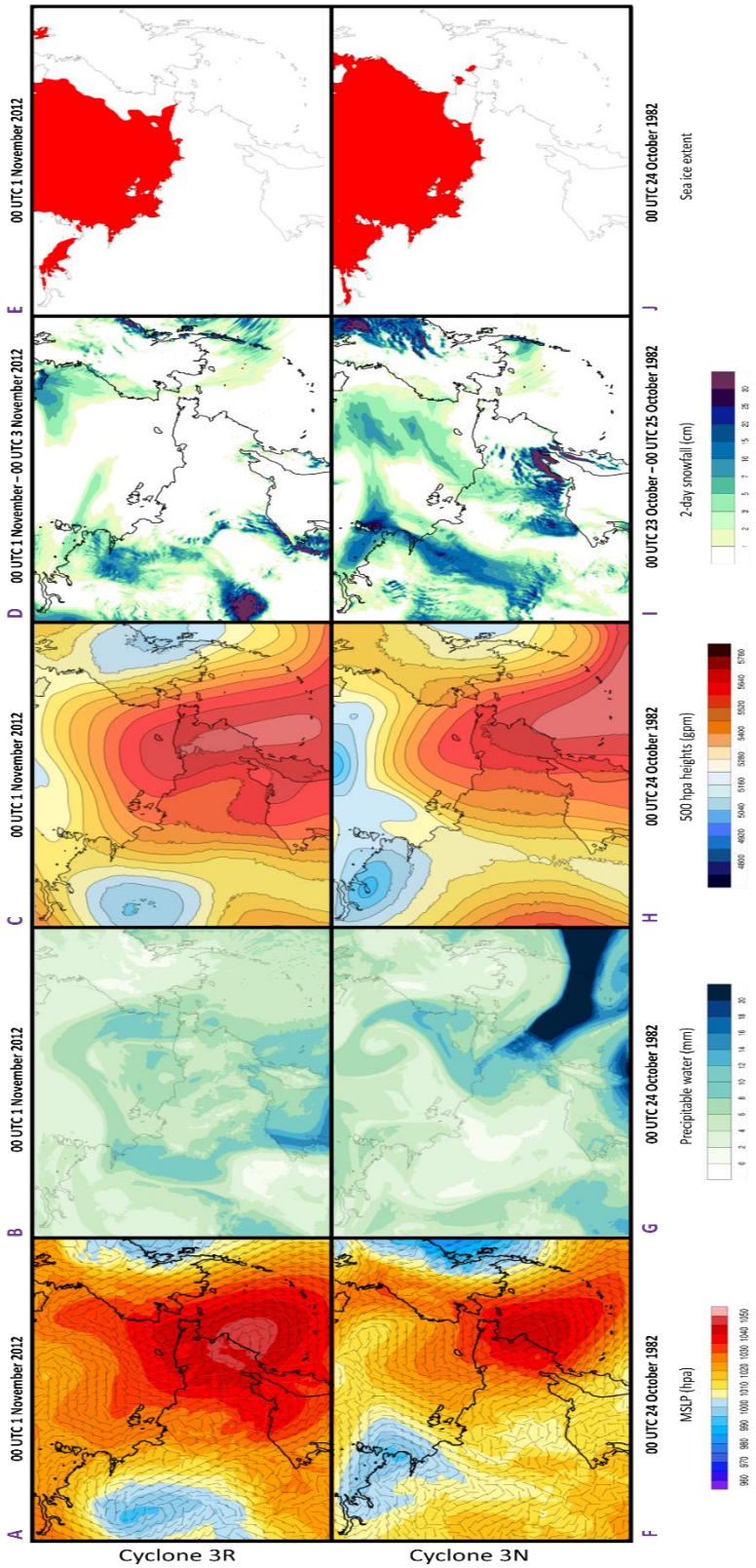

Figure 4.13.
Case study 3, for cyclones occurring on 00 UTC 1 November 2012 – 00 UTC 3 November 2012 and 00 UTC 23 October 1982 – 00 UTC 25 October 1982. MSLP/wind vectors (A and F), precipitable water (B and G), 500 hpa heights (C and H), total accumulated snowfall (D and I), and sea ice extent (E and J) are displayed

A

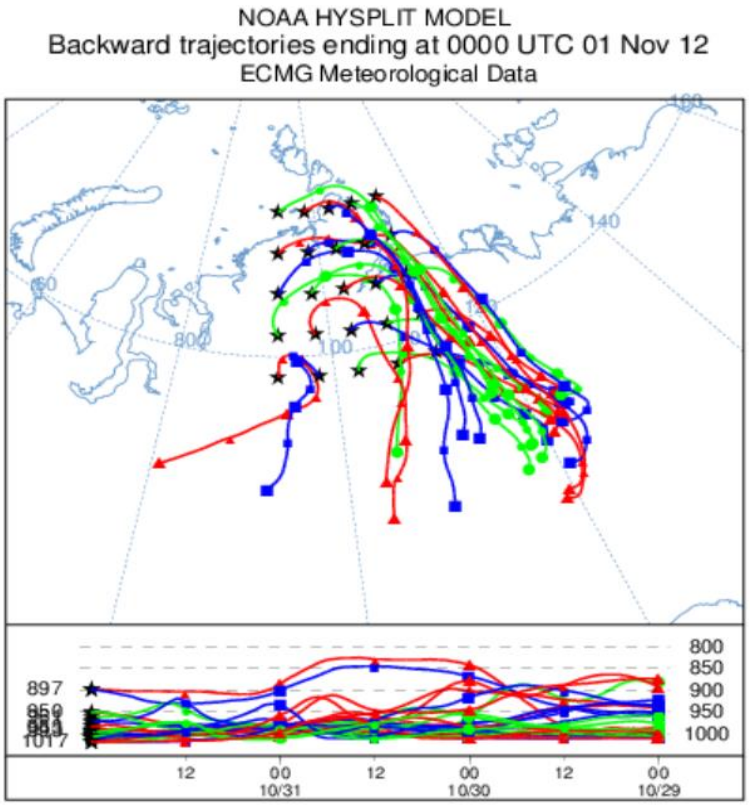

B

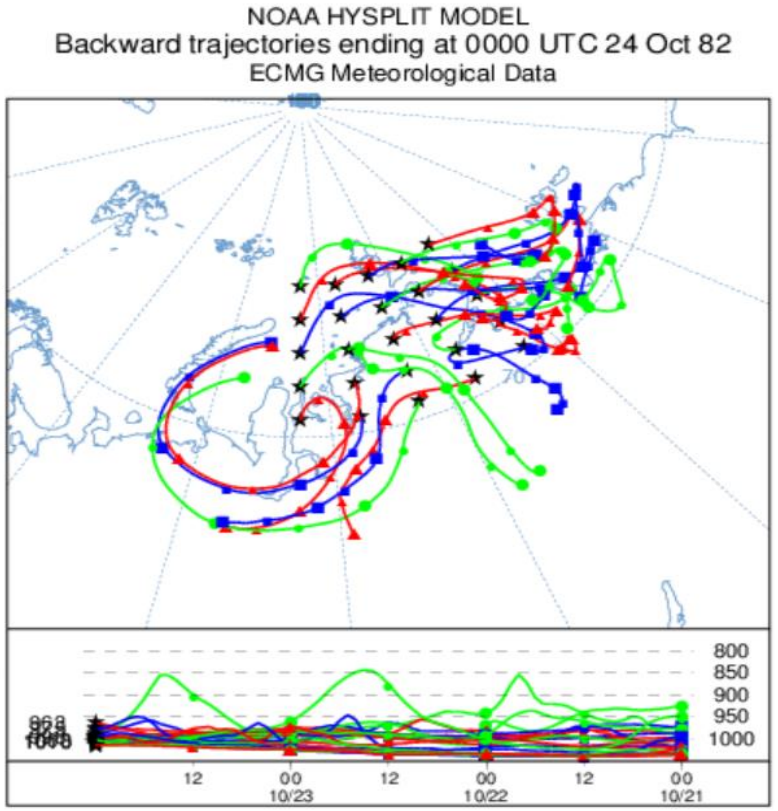

Figure 4.14.

HYSPLIT 72 hour back-trajectory analysis for Cyclone 3R (A) and Cyclone 3N (B), the varied colors of the HYSPLIT back-trajectories hold no importance other than allowing for an easier distinction between the parcel trajectories

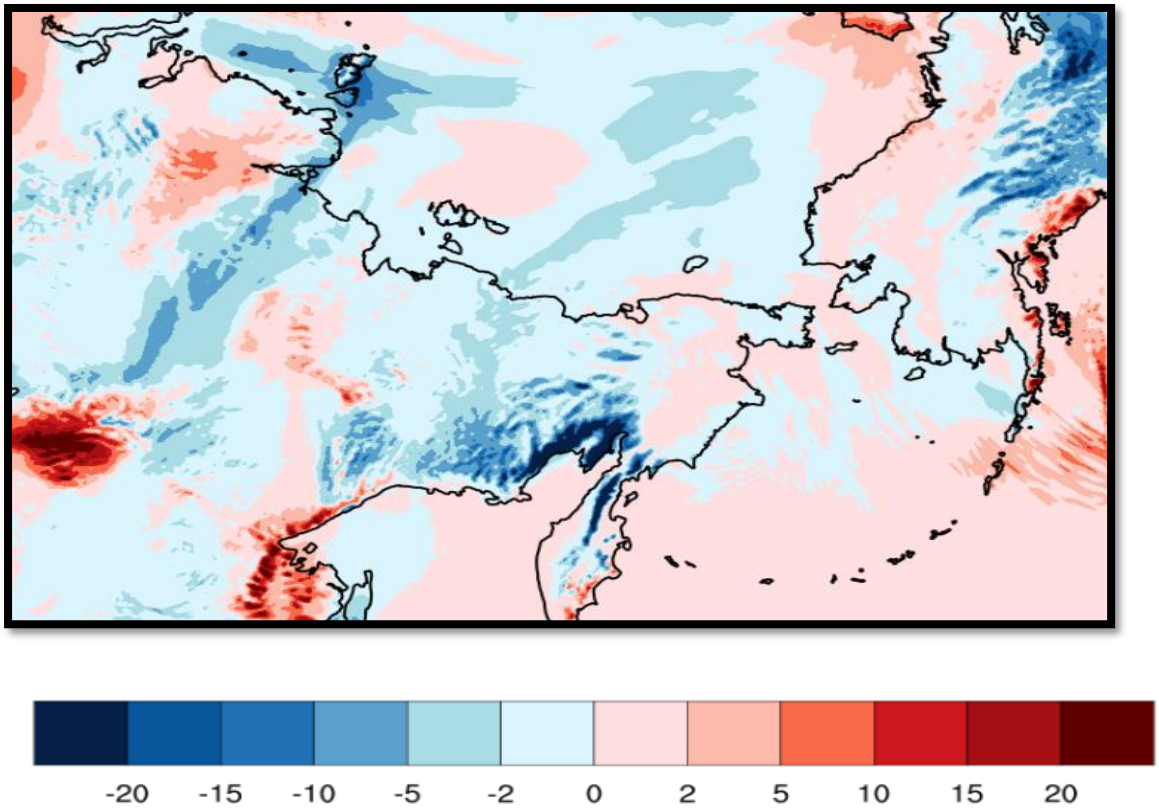

Figure 4.15.

Difference in snowfall (cm) occurring between cyclone 3R and cyclone 3N (cyclone 3R – cyclone 3N)

4.3 **Discussion**

Cases 1 and 2 support the hypothesis, with Cyclones 1R and 2R producing enhanced snowfall in a reduced Arctic sea ice extent environment, while Cyclones 1N and 2N produce lesser snowfall in an environment with greater sea ice extent. Case 3 produces greater snowfall in Cyclone 3N in an environment with greater sea ice extent than Cyclone 3R, failing to support the hypothesis.

If declining sea ice is causing an increase in snow precipitation across the Arctic, it should be accompanied by an increase in moisture. Looking at the precipitable water plots for the cases (Figures 4.7, 4.10, 4.13 B and G), it appears that a slight increase in moisture occurs between the reduced to normal sea ice extent years within the vicinity of the cyclones investigated. In Case 1, the moisture increases over the ice-free regions of the Arctic do not migrate far from the open waters of the Arctic. This leads to more snowfall occurring over the ocean and along coastal regions of Alaska. In Case 2, the higher moisture is advected northward over the sea ice and away from the open Arctic waters. This allows for enhanced snowfall to occur both over the open waters of the Arctic Ocean and over a large extent of sea ice coverage to the north, where it can accumulate on the ice. An increase in available moisture does not guarantee an increase in precipitation within an individual cyclone, as was shown in Case 3; however, if other factors are favorable, an increase in moisture could lead to greater snowfall.

The results of Cyclone 1R and Cyclone 2R both produce enhanced snowfall under a reduced sea ice environment, though they create different impacts on regional snow depth. Some of the snowfall that occurs in Cyclone 1R will not accumulate, as the snow will fall over open waters. If the snowfall is not accumulating, snow depth increases and

resulting impacts to the local climate will not occur. Coastal locations in Alaska receive greater snowfall in Cyclone 1R, and therefore an increase in snow depth. The highest snowfall in Cyclone 2R extends over the sea ice-covered regions of the high Arctic. Snowfall in this case will accumulate on top of the sea ice, increasing snow depth, and leading to an impact on the regional climate. The maximum snowfall in Cyclone 2R extends much further away from the open waters of the Arctic Ocean than the snowfall in Cyclone 1R. This leads to a larger geographical coverage of accumulating snowfall in Cyclone 2R than in Cyclone 1R.

Two possible factors may contribute to the differences in snowfall and moisture advection between Cyclones 1R and 2R. The first possible factor is that the moisture advection in Cyclone 2R is occurring on the east side of the cyclone, where the meridional-component of the wind flow is from the south. The air here is likely warmer, and can hold more moisture. This is seen when looking at the precipitable water for the two cases (Figures 4.7, 4.10, 4.13 B and G), where Cyclone 2R possesses greater moisture over the east and north side of the cyclone, compared to the northwestern region of the cyclones experiencing snowfall in Cyclone 1R. A second potential factor that could lead to differing moisture advection between Cyclones 1R and 2R are the forcing mechanisms causing the snowfall. The maximum snowfall in Cyclone 2R occurs to the north of the cyclone, near the North Pole. This is the region of the cyclone where a deformation zone would set up, where forcing occurs due to mid-level warm air advection. The moisture resulting from a decrease in Arctic sea ice would advect northward and rise vertically, supporting snowfall to the north. The snowfall in Cyclone 1R looks to occur due to cold air advection over relatively warmer ocean waters,

generating instability in the lower layers of the atmosphere. When the air moves onto land, the atmosphere stabilizes, shutting off the snowfall. This could prevent the snowfall from penetrating very far into the Alaskan mainland.

Case 3 shows that a decrease in sea ice will not always foster greater snowfall within a cyclone, and serves as a reminder that there are many other factors that impact the amount of snowfall that occurs within a high-latitude cyclone. Although Case 3 does not support the hypothesis, it still provides an example of a case that goes against expectations, and allows for an exploration into the variables that may prevent a decrease in sea ice decline from leading to greater snowfall. Differing temperature, forcings for ascent or other variables may prevent Cyclone 3R from producing greater snowfall than Cyclone 3N in Case 3. It may also be possible that the increases in heat and moisture fluxes due to a lesser sea ice extent with Cyclone 3R do not have a large impact on snowfall.

CHAPTER 5: CONCLUSIONS

This study considers the impact of a reduced autumnal Arctic sea ice extent on snowfall occurring within high-latitude cyclones, attempting to show that snowfall will increase with a decrease in sea ice extent. A case study analysis is conducted to investigate snowfall occurring within cyclones over differing sea ice environments, along with a monthly snowfall and snow cover analysis to observe how snowfall changes at a seasonal time scale. A relationship likely exists between declining sea ice and snowfall produced by high-latitude cyclones. The modeled results from Cases 1 and 2 display an increase in moisture in regions of ice-free waters within the Arctic Ocean, yielding greater snowfall in ice-free oceanic regions. The results of these cases suggest that coastal locations, along with ice-covered regions near the sea ice margin, have the greatest potential for increased snow depth and an impact on the regional climate. Case 3 demonstrates that a decrease in sea ice will not always lead to an increase in snowfall within a high-latitude cyclone, as there is a potential for variables such as temperature and forcing for ascent to have a greater impact on snowfall production than moisture.

The results from the monthly snowfall analysis suggest that monthly snowfall is greater in the reduced sea ice extent years than the normal sea ice extent years over the Arctic Ocean in October. The snow depth analysis reveals that by the end of November, snow depth is greater in the reduced sea ice extent years than the normal sea ice extent years over multi-year sea ice near the North Pole, while snow depth is less across the rest of the Arctic Ocean in the reduced sea ice extent years. Continental regions have noisy results for the monthly snowfall and snow depth analysis, though the case study analyses

suggest that there is a potential for snowfall to increase along coastal regions due to sea ice decline.

The regions prone to increasing snowfall may experience a variety of impacts. Coastal locations in Siberia and Alaska that observe greater snow depth could see decreasing temperature (Krasting et al. 2013), increasing ice mass over glaciated terrain (Singarayer et al. 2006), and increasing freshwater runoff (Bengtsson et al. 2011) during the melt season. Increases in snow depth that occur over sea ice could lead to a decrease in ice thickness during the cold season, as well as increased ice thickness and coverage during the spring and summer melt season (Hezel et al. 2012). These impacts are relative to the ambient warming occurring with global climate change.

The utilization of a model in this study leaves some room for error in the projected snowfall in the cyclone cases. Additionally, some of the moisture increases in the ice-free regions of the Arctic may be a result of temperature increases and the Clausius-Clapeyron relationship. These factors, along with a limited sample size of three cases, demand that caution be taken in making conclusions. Though this study does not conclusively demonstrate that decreasing sea ice extent will increase snowfall within high-latitude cyclones, it provides enough evidence for a relationship between sea ice extent and snowfall to warrant further research. The testing of additional cases may be necessary to further increase confidence in the results. The year 2016 had the lowest sea ice extent on record in late October and November. This period also saw anomalously high snowfall across much of the Siberia, and may be a good period to draw an additional case. This study can also be conducted with a prescribed sea ice environment, investigating the results of a cyclone within an environment with zero sea ice (as will

likely happen in the future). Additionally, this study could be conducted utilizing data from surface observations if an Arctic surface observational dataset with greater coverage becomes available in the future.

This study pioneers a sector of climate research that has lacked attention. It is important for climatologists to get a better knowledge of the smaller scale feedbacks to climate change, many of which are poorly understood. These feedbacks may hold the key to understanding the changes that will occur in the future Arctic climate system. As atmospheric greenhouse gas concentrations continue to rise, the Earth is going to continue warming, and greater changes are going to occur within the Arctic climate. Warm-season Arctic sea ice will continue to decline in the future, making it important to gain a better understanding of feedbacks occurring due to Arctic sea ice decline.

REFERENCES

Alexander, M. A., U. S. Bhatt, J. E. Walsh, M. S. Timlin, J. S. Miller, and J. D. Scott, 2004: The atmospheric response to realistic Arctic sea ice anomalies in an AGCM during winter. *J. Climate*, **17**,890–905, doi:10.1175/15200442(2004)017<0890:TARTRA>2.0.CO;2

Beesley, J. A., 2000: Estimating the effect of clouds on the surface energy balance. *Geophys. Res. Lett.*, **105,** 10,103-110,117.

Bengtsson, L., K. I. Hodges, S. Koumoutsaris, M. Zahn, and N. Kennlyside, 2011: The changing atmospheric water cycle in polar regions in a warmer climate. *Tellus,* **63A**, 907-920, doi:10.1111/j.1600-0870.2011.00534.x.

Bromwich, D. H., 2017: The Arctic system reanalysis. *14th conference on Polar Meteorology and Oceanography*, Seattle, WA

Cohen, J. L., J. C. Furtando, M. A. Barlow, V. A. Alexeev, J. E. Cherry, 2012: Arctic warming, increasing snow cover and widespread boreal winter cooling. *Enviorn. Res. Lett.*, **7**, 011004, doi:10.1088/1748-9326/7/1/014007

Dee, D., and Coauthors, 2011: The ERA-Interim reanalysis: Configuration and performance of the data assimilation system. *Quart. J. Roy. Meteor. Soc*., **137**, 553–597, doi:10.1002/qj.828.

DeRepentigny, P., L. B. Tremblay, R. Newton, and S. Pfirman, 2016: Patterns of sea ice retreat in the transition to a seasonally ice-free arctic. *J. Climate*, **29**, 6993-7008, doi: 10.1175/JCLI-D-15-0733.1.

Deser, C., R. Tomas, M. Alexander, and D. Lawrence, 2010: The seasonal atmospheric response to projected arctic sea ice loss in the late twenty-first century. *J. Climate*, **23**, 333–351.doi: http://dx.doi.org/10.1175/2009JCLI3053.1

Eastman, R., and S. G. Warren, 2010: Interannual variations of Arctic cloud types in relation to sea ice. *J. Climate*, **23**, 4216–4232, doi:10.1175/2010JCLI3492.1

Fiorino, M., 2004: A multi-decadal daily sea surface temperature and sea ice concentration data set for the ERA-40 reanalysis. *ERA-40 Project Report Series No. 12, ECMWF*, Reading, UK

Francis, J. A., W. Chan, D. J. Leathers, J. R. Miller, and D. E. Veron, 2009: Winter Northern Hemisphere weather patterns remember summer Arctic sea-ice extent. *Geophys. Res. Lett.*, **36**, L07503, doi:10.1029/2009GL037274.

Hezel, P. J., X. Zhang, C. M. Bitz, B. P. Kelly, and F. Massonnet, 2012: Projected decline in spring snow depth on Arctic sea ice caused by progressively later autumn open ocean freeze-up this century. *Geophys. Res. Let.*, **39**, L17505, doi:10.1029/2012GL052794.

Hinzman, L. D., and coauthors, 2005: Evidence and implications of recent climate change in northern Alaska and other arctic regions. *Climatic Change*, **72,** 251-298Holland, M., 2003: The North Atlantic Oscillation–Arctic Oscillation in the CCSM2 and its influence on Arctic climate variability. *J. Climate*, **16**,2767–2781.

Kapnick, S., and T. Delworth, 2013: Controls of global snow under a changed climate. *J. Climate*, **26**, 5537–5562, doi:10.1175/JCLI-D-12-00528.1.Krasting, J., A. Broccoli, K. Dixon, and J. Lanzante, 2013: Future changes in Northern Hemisphere snowfall. *J. Climate*, **26**, 7813–7828, doi:10.1175/JCLI-D-12-00832.1

Kurita, N., 2011: Origin of Arctic water vapor during the ice-growth season. *Geophys. Res. Lett.*, **38**, L02709, doi: 10.1029/2010GL04064

Liston, G. E., and C. A. Hiemstra, 2011: The Changing Cryosphere: Pan-Arctic Snow Trends (1979–2009). *J. Climate*, **24**, 5691-5712

Lindsay, R. W., and J. Zhang, 2005: The thinning of Arctic sea ice, 1988–2003: Have we passed a tipping point? *J. Climate*, **18**, 4879–4894, doi:10.1175/JCLI3587.1

Liua, J., J. A. Curry, H. Wang, M. Song, and R. M. Horton, 2012: Impact of declining Arctic sea ice on winter snowfall. *PNAS*, **109**, 11, 4074-4079. doi: 10.1073/pnas.1114910109

National Centers for Environmental Information, 2017: Climate at a Glance, Accessed 11 June 2017. [Available online at https://www.ncdc.noaa.gov/cag/]

National Centers for Enviornmental Information, 2017: Climate change and variability, Accessed 23 July 2017. [Available online at https://www.ncdc.noaa.gov/climate-information/climate-change-and-variability]

National Snow and Ice Data Center, 2017: Charctic Interactive Sea Ice Graph, Accessed 11 June 2017. [Available online at http://nsidc.org/arcticseaicenews/charctic-interactive-sea-ice-graph/]

National Snow and Ice Data Center, 2017: Sea Ice Index, Accessed 13 November 2017.[Available online at https://nsidc.org/data/seaice_index/archives/image_select.html]

Parkinson, C. L., 2014: Global Sea Ice Coverage from Satellite Data: Annual Cycle and 35-Yr Trends. *J. Climate*, **27**, 9377–9382.

Räisänen, J., 2008: Warmer climate: less or more snow? *J. Clim dyn.*, **30,** 307-319

Rolph, G., A. Stein, and B. Stunder, 2017: Real-time environmental applications and display system: READY. *Environmental Modelling & Software*, **95**, 210-228,

Schweiger, A. J., R.W. Lindsay, S Vavrus, and J. A. Francis, 2008: Relationships between Arctic Sea Ice and Clouds during Autumn. *J. Climate*, **21**, 4799-4810. Screen, J. A., I. Simmonds, C. Deser, and R. Tomas, 2013: The atmospheric response to three decades of observed Arctic sea ice loss. *J. Climate*, **26**, 1230–1248, doi:10.1175/JCLI-D-12-00063.1.

Sedláček, J., R. Knutti, O. Martius, and U. Beyerle, 2012: Impact of a reduced arctic sea ice cover on ocean and atmospheric properties. *J. Climate,* **21**, 307-319.

Seefeldt, M. W., M. Tice, J. J. Cassano, and M. D. Shupe, 2012: Evaluation of WRF Radiation and Microphysics Parameterizations for use in the Polar Regions. *Atmospheric Model Parameterizations in the Polar Regions Workshop,* Boulder, CO

Simmonds, I., and K. Keay, 2009: Extraordinary September Arctic sea ice reductions and their relationships with storm behavior over 1979-2008. *Geophys. Res. Lett.*, **36**, L19715, doi:10.1029/2009GL039810.

Simmonds, I, and J. A. Screen, 2010: The central role of diminishing sea ice in recent Arctic temperature amplification. *Nature*, **464**, 1334-1337, doi:10.1038/nature09051

Singarayer, J., J. Bamber, and P. Valdes, 2006: Twenty-first-century climate impacts from a declining Arctic sea ice cover. *J. Climate*, **19**, 1109–1125, doi:10.1175/JCLI3649.1.

Skamarock, W. C., J. B. Klemp, J. Dudhia, D. O. Gill, D. M. Barker, M. G Duda, X.-Y. Huang, W. Wang, and J. G. Powers, 2008: A Description of the Advanced Research WRF Version 3. *NCAR Tech. Note NCAR/TN-475+STR*, 113 pp. doi:10.5065/D68S4MVHSorteberg, A., and B. Kvingedal, 2006: Atmospheric forcing on the Barents Sea winter ice extent. *J. Climate*, **19**,4772–4784, doi:10.1175/JCLI3885.1

Stein, A. F., R.R. Draxler, G. D. Rolph, B. J. B. Stunder, M. D. Cohen, and F. Ngan, 2015: NOAA's HYSPLIT atmospheric transport and dispersion modeling system. *Bull. Amer. Meteor. Soc.*, **96**, 2059-2077, http://dx.doi.org/10.1175/BAMS-D-14-00110.1

Stone, R. S., E. G. Dutton, J. M. Harris, and D. Longenecker, 2002: Earlier spring snowmelt in northern Alaska as an indicator of climate change. *J. Geophys. Res.*, 107(D10)

Strey, S. T., W. L. Chapman, and J. E. Walsh, 2010: The 2007 sea ice minimum: impacts on the Northern Hemisphere atmosphere in late autumn and early winter. *Geophys. Res. Lett.*, **115**, D23103, doi:10.1029/2009JD013294

Stroeve, J. C., T. Makus, L, Boisvert, J. Miller, and A. Barrett, 2014: Changes in Arctic melt season and implications for sea ice loss. *Geophys. Res. Lett.*, **41,** 1216-1225, doi:10.1002/2013GL05895 1

Warren, S. G., I. G. Rigor, N. Untersteiner, V. F. Radionov, N. N. Bryazgin, Y. I. Aleksandrov, and R.Colony, 1999: Snow depth on arctic sea ice. *J. Climate*, **12**, 1814–1829, doi:10.1175/1520-0442(1999)012<1814:SDOASI>2.0.CO;2.

Wegmann, M., and coauthors, 2015: Arctic moisture source for Eurasian snow cover variations in autumn. *Enviorn. Res. Lett*., 10, 1-10, doi: 10.1088/1748-9326/10/5/054015

Wu, W., J. Su, and R. Zhang, 2011: Effects of autumn-winter Arctic sea ice on winter Siberian High. *Chin. Sci. Bull.*, **56,** No.30: 3220-3228, doi:10.1007/s114-011-4696-4

Yin, J., H., 2005: A consistent shift of the storm tracks in simulations of 21st century climate. *Geophys. Res. Lett.*, **32**: L18701, doi:10.1029/2005GL023684

Zhang, X., J. E. Walsh, J. Zhang, U. S. Bhatt, and M. Ikeda, 2004: Climatology and interannual variability of Arctic cyclone activity: 1948–2002. *J. Climate*, **17**, 2300–2317, doi:10.1175/1520-0442(2004)017<2300:CAIVOA>2.0.CO;2.

Appendix: WRF namelist file

```
&time_control
 run_days                            = 0,
 run_hours                           = 0,
 run_minutes                         = 0,
 run_seconds                         = 0,
 start_year                          = 1982, 1982, 1982,
 start_month                         = 10,   10,   10,
 start_day                           = 30,   30,   30,
 start_hour                          = 00,   00,   00,
 start_minute                        = 00,   00,   00,
 start_second                        = 00,   00,   00,
 end_year                            = 1983, 1983, 1983,
 end_month                           = 01,   01,   01,
 end_day                             = 02,   02,   02,
 end_hour                            = 00,   00,   00,
 end_minute                          = 00,   00,   00,
 end_second                          = 00,   00,   00,
 interval_seconds                    = 21600
 input_from_file                     =
.true.,.true.,.true.,.true.,.true.,.true.,.true.,
 fine_input_stream                   = 2,2,2,2,2,2,2,
 history_interval                    = 180, 180, 180, 180,180,180,180,
 frames_per_outfile                  = 8, 8, 8, 8, 8, 8,8,
 restart                             = .true.,
 restart_interval                    = 14400
 io_form_history                     = 2
 io_form_restart                     = 2
 io_form_input                       = 2
 io_form_boundary                    = 2
 debug_level                         = 0
 auxinput4_inname                    = "wrflowinp_d<domain>"
 auxinput4_interval                  = 360,360,360,360,360,360,360,
 io_form_auxinput4                   = 2
 io_form_auxinput2                   = 2
 write_hist_at_0h_rst                = .true.
 adjust_output_times                 = .true.
 override_restart_timers             = .true.
 /

 &domains
 time_step                           = 180,
 time_step_fract_num                 = 0,
 time_step_fract_den                 = 1,
 max_dom                             = 2,
 e_sn          = 133,352,
 e_we          = 183,502,
 e_vert                              = 30,   30,  30,
```

```
 num_metgrid_levels                  = 38,
 num_metgrid_soil_levels             = 4,
 dx                                  = 36000, 12000, 4000,
 dy                                  = 36000, 12000,4000,
 grid_id                             = 1,     2,     3,
 parent_id                           = 0,     1,     2,
 i_parent_start    = 1,8,
 j_parent_start    = 1,8,
 parent_grid_ratio                   = 1,     3,     3, 3, 3,3,3,
 parent_time_step_ratio              = 1,     3,     3, 3, 3,3,3,
 feedback                            = 0,
 smooth_option                       = 0,
 use_adaptive_time_step              = .true.
 step_to_output_time                 = .true.
 target_cfl                          = 1.0,    1.0,     1.0,
 max_step_increase_pct               =   5,     75,      75,
 starting_time_step                  =  180,    90,      60,
 max_time_step                       = 450,     -1,     -1,
 min_time_step                       = 60,     -1,    20,
 adaptation_domain                   = 2
 target_hcfl                         = 0.84, 0.84, 0.84,0.84, 0.84,
0.84,0.84,
 /


 &physics
 surface_input_source                = 1,
 sst_update                          = 1
 usemonalb                           = .true.,
 rdmaxalb                            = .true.,
 mp_physics                          = 7,     7,     7,7,7,7,7,
 ra_lw_physics                       = 1,     1,     1,1,1,1,1,
 ra_sw_physics                       = 2,     2,     2,2,2,2,2,
 radt                                = 20,    20,    20,20, 20,20,20,
 sf_sfclay_physics                   = 2,     2,     2,2,2,2,2,
 sf_surface_physics                  = 2,     2,     2,2,2,2,2,
 bl_pbl_physics                      = 2,     2,     2,2,2,2,2,
 bldt                                = 0,     0,     0,0,0,0,0,
 cu_physics                          = 3,     3,     3,3,3,3,3,
 fractional_seaice                   = 1,
 seaice_threshold                    = 0,
 cudt                                = 5,     5,     5,5,5,5,5,
 isfflx                              = 1,
 ifsnow                              = 0,
 icloud                              = 1,
 num_soil_layers                     = 4,
 sf_urban_physics                    = 0,     0,     0,0,0,0,0,
 maxiens                             = 1,
 maxens                              = 3,
 maxens2                             = 3,
```

```
 maxens3                             = 16,
 ensdim                              = 144,
 /
iz0tlnd                             = 1,


 &fdda
  /

 &dynamics
 w_damping                           = 1,
 diff_opt                            = 1,
 km_opt                              = 4,
 diff_6th_opt                        = 0,      0,      0,0,0,0,0,
 diff_6th_factor                     = 0.12,   0.12,
0.12,0.12,0.12,0.12,0.12,
 base_temp                           = 290.
 damp_opt                            = 3,
 zdamp                               = 5000.,  5000.,
5000.,5000.,5000.,5000.,5000.,
 dampcoef                            = 0.2,    0.2,
0.2,0.2,0.2,0.2,0.2,
 khdif                               = 0,      0,      0,0,0,0,0,
 kvdif                               = 0,      0,      0,0,0,0,0,
 non_hydrostatic                     = .true., .true.,
.true.,.true.,true.,.true.,.true.,
 moist_adv_opt                       = 1,      1,      1, 1,1,1,
 scalar_adv_opt                      = 1,      1,      1, 1,1,1,
 use_baseparam_fr_nml                =.t.
 /

 &bdy_control
 spec_bdy_width                      = 5,
 spec_zone                           = 1,
 relax_zone                          = 4,
 specified                           = .true.,
.false.,.false.,.false.,.false.,.false.,false.,
 nested                              = .false., .true., .true.,.true.,
.true.,.true.,.true.,
 /

 &grib2
 /

 &namelist_quilt
 nio_tasks_per_group = 0,
 nio_groups = 1,
```